BIT SYNCHRONIZATION SYSTEM PERFORMANCE CHARACTERIZATION, MODELING, AND TRADE-OFF STUDY

W. C. Lindsey

University of Southern California

Prepared for:

Naval Missile Center

4 September 1973

Technical Publication TP-73-18

BIT SYNCHRONIZATION SYSTEM PERFORMANCE CHARACTERIZATION, MODELING, AND TRADEOFF STUDY

(AIRTASK A5355352-054E-3F09905003)

By

W. C. LINDSEY
University of Southern California
(Contract N61756-72-M-6443)

4 September 1973

NAVAL MISSILE CENTER

Point Mugu, California

TP-73-18 (U)

90 e

UNCLASSIFIED

SECURITY CLASSIFICATION OF THIS PAGE (When Data Entered)

REPORT DOCUMENTATION PAGE		READ INSTRUCTIONS BEFORE COMPLETING FORM
1. REPORT NUMBER TP-73-18	2. GOVT ACCESSION NO.	3. RECIPIENT'S CATALOG NUMBER
4. TITLE (and Subtitle) BIT SYNCHRONIZATION SYSTEM PERFORMANCE CHARACTERIZATION, MODELING, AND TRADEOFF STUDY		5. TYPE OF REPORT & PERIOD COVERED 6. PERFORMING ORG. REPORT NUMBER
7. AUTHOR(s) W. C. Lindsey		8. CONTRACT OR GRANT NUMBER(s) Contract N61756-72-M-6443
9. PERFORMING ORGANIZATION NAME AND ADDRESS University of Southern California Los Angeles, California 90007		10. PROGRAM ELEMENT, PROJECT, TASK AREA & WORK UNIT NUMBERS AIRTASK A5355352-054E-3F09905003
11. CONTROLLING OFFICE NAME AND ADDRESS Naval Missile Center (Code 5630) Point Mugu, California 93042		12. REPORT DATE 4 September 1973 13. NUMBER OF PAGES<br~~81~~ 96
14. MONITORING AGENCY NAME & ADDRESS (if different from Controlling Office)		15. SECURITY CLASS. (of this report) UNCLASSIFIED 15a. DECLASSIFICATION, DOWNGRADING SCHEDULE

16. DISTRIBUTION STATEMENT (of this Report)

Approved for public release; distribution unlimited.

17. DISTRIBUTION STATEMENT (of the abstract entered in Block 20, if different from Report)

18. SUPPLEMENTARY NOTES

19. KEY WORDS (Continue on reverse side if necessary and identify by block number)

Bit decision
Bit synchronization
PCM (pulse code modulation)
PCM signal conditioner

20. ABSTRACT (Continue on reverse side if necessary and identify by block number)

This report presents the results obtained during the study on mathematical modeling of PCM bit synchronizers (also known as PCM signal conditioners). It is written in two parts. The first part presents results obtained on the study of the effects which bit synchronization has on the bit error rate (BER). Several PCM baseband signaling formats are included in the study, viz., RZ, NRZ, Manchester, and Miller Coding. Theoretical performance limitations of bit synchronizers and the

Continued

DD FORM 1 JAN 73 1473 EDITION OF 1 NOV 65 IS OBSOLETE

UNCLASSIFIED

SECURITY CLASSIFICATION OF THIS PAGE (When Data Entered)

20. ABSTRACT (Concluded)

associate bit detector are developed by relating the BER to the signal-to-noise ratio per bit. It is assumed that the noise added to the input signal is white and Gaussian, the PCM signal waveforms are either rectangular or filtered and that bit synchronization is perfect. Next the constraint of perfect bit sync is relaxed to include the more practical case where bit sync jitter and bit slippage affect the detection of the data bits. To account for the effects of bit sync jitter on the BER, the probability density function of bit sync jitter, valid for a broad class of bit synchronization systems (BSS), is postulated and this is interconnected with the theory of bit detection. The deleterious effects are described in terms of the parameter $\sigma_\tau = T\sigma_\lambda$; where σ_λ represents the nomalized bit sync jitter and T is bit duration in seconds. Various design curves and performance comparisons are made for several PCM baseband signaling formats.

The second part of this report is devoted to the study of bit synchronization performance characterization. A general discussion is given which highlights the many performance measures which serve to characterize the performance of BSS. Some general mathematical relations are given for evaluation of the acquisition time, acquisition range, and bit slippage rate for PCM bit synchronizers which are mechanized such that the phase detector characteristic is periodic.

This theory is followed by a discussion of bit synchronizer performance comparisons and this leads to the suggestion of the mathematical models which can be implemented using the method of computer software. The four parameters of interest in the computer software model include bit sync acquisition time, bit slippage rate, bit sync jitter and bit sync acquisition range. Two bit sync approaches which will lead to a specific software package are recommended: These include the absolute value, least squares and decisions directed approach. The approach leads to suggestions of techniques which can be used in the procurement of BSS as well as the development of standard procedures for testing PCM BSS.

ACKNOWLEDGMENTS

The author wishes to thank Messrs. Kenneth Berns, Franklin R. Hartzler, Eugene R. Hill, and James L. Weblemoe of the Naval Missile Center for offering helpful comments and participating in numerous discussions during the course of this study.

The author also wishes to thank the publisher for permission to quote from Synchronization Systems in Communications and Control, by William C. Lindsey, (c) 1972, by Prentice-Hall, Inc., Englewood Cliffs, N.J.

The author also wishes to thank the Institute of Electrical and Electronics Engineers, Inc., 345 East 47th Street, New York, N.Y., for permission to reprint material from IEEE Transactions on Communications Technology, Volumes COM-15; COM-17, No. 3; and COM-18, No. 3.

FOREWORD

Work on the characterization and mathematical modeling of classes of PCM Bit Synchronizers was conducted under AIRTASK A5355352-054E-3F09905003 to provide technical support to the Telemetry Group of the RCC (Range Commanders Council). The work is part of Work Unit Assignment A535210000002, Range Telemetry Support. The purpose of the task is to conduct a program of testing and investigation that will provide information which can be used by the Telemetry Group to keep the RCC publications of "Telemetry Standards" and "Test Methods for Telemetry Systems and Subsystems" updated and abreast of technological advances.

The investigations were conducted and the report prepared by Dr. William C. Lindsey, University of Southern California, under Navy contract N61756-72-M-6443.

T. B. JACKSON
Head, Data Systems Division

CONTENTS

CONTENTS (Continued)

CONTENTS (Concluded)

NAVAL MISSILE CENTER
Point Mugu, California

TP-73-18
4 September 1973

BIT SYNCHRONIZATION SYSTEM PERFORMANCE CHARACTERIZATION, MODELING, AND TRADEOFF STUDY

(AIRTASK A5355352-054E-3F09905003)

By
W. C. LINDSEY

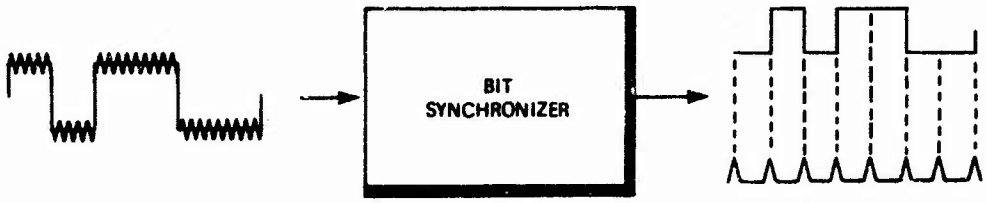

SUMMARY

This report presents the results obtained during the study on mathematical modeling of PCM bit synchronizers (also known as PCM signal conditioners). It is written in two parts. The first part presents results obtained on the study of the effects which bit synchronization has on the bit error rate (BER). Several PCM baseband signaling formats are included in the study, viz., RZ, NRZ, Manchester, and Miller Coding. Theoretical performance limitations of bit synchronizers and the associate bit detector are developed by relating the BER to the signal-to-noise ratio per bit. It is assumed that the noise added to the input signal is white and Gaussian, the PCM signal waveforms are either rectangular or filtered and that bit synchronization is perfect. Next the constraint of perfect bit sync is relaxed to include the more practical case where bit sync jitter and bit

slippage affect the detection of the data bits. To account for the effects of bit sync jitter on the BER, the probability density function of bit sync jitter, valid for a broad class of bit synchronization systems (BSS), is postulated and this is interconnected with the theory of bit detection. The deleterious effects are described in terms of the parameter $\sigma_\tau = T\sigma_\lambda$; where σ_λ represents the normalized bit sync jitter and T is bit duration in seconds. Various design curves and performance comparisons are made for several PCM baseband signaling formats.

The second part of this report is devoted to the study of bit synchronization performance characterization. A general discussion is given which highlights the many performance measures which serve to characterize the performance of BSS. Some general mathematical relations are given for evaluation of the acquisition time, acquisition range, and bit slippage rate for PCM bit synchronizers which are mechanized such that the phase detector characteristic is periodic.

This theory is followed by a discussion of bit synchronizer performance comparisons and this leads to the suggestion of the mathematical models which can be implemented using the method of computer software. The four parameters of interest in the computer software model include bit sync acquisition time, bit slippage rate, bit sync jitter and bit sync acquisition range. Two bit sync approaches which will lead to a specific software package are recommended: These include the absolute value, least squares and decisions directed approach. The approach leads to suggestions of techniques which can be used in the procurement of BSS as well as the development of standard procedures for testing PCM BSS.

Publication Unclassified.

I. THEORETICAL PERFORMANCE OF IDEAL PCM SIGNAL CONDITIONERS*

In this part we consider the problem of detecting two equally probable signal waveforms $s_1(t)$ or $s_2(t)$, each of duration T seconds, in a background of white Gaussian noise of single-sided spectral density of N_0 watts/Hz. The various PCM signaling formats to be considered are illustrated in Fig. I-1.

Now suppose that in each of a succession of time intervals of duration T we know that the received signal consists of either signal $s_1(t)$ or $s_2(t)$ and additive noise, say n(t). We seek a data detector (wherein bit sync is assumed known) that will decide on the basis of the received waveform in each interval which of the two possible signals was transmitted. If we choose the <u>figure of merit</u> for such a device to be the error probability then the optimum (perfectly synchronized) data detector is one that will announce $s_1(t)$ if

$$\frac{1}{T}\int_0^T [x(t) - s_1(t)]^2 dt < \frac{1}{T}\int_0^T [x(t) - s_2(t)]^2 dt \qquad (I\text{-}1)$$

Here x(t) represents the received signal plus noise. Assuming $s_1(t)$ and $s_2(t)$ have equal energy i.e.,

$$E \triangleq \int_0^T s_1^2(t)dt = \int_0^T s_2^2(t)dt = ST \qquad (I\text{-}2)$$

we can expand the integrands and cancel common terms to obtain the equivalent decision rule: Announce $s_1(t)$ present if

$$\int_0^T x(t)s_1(t)dt > \int_0^T x(t)s_2(t)dt \qquad (I\text{-}3)$$

*In this report the term "signal conditioner" is used to imply the bit detector and bit synchronizer as a combined operational system.

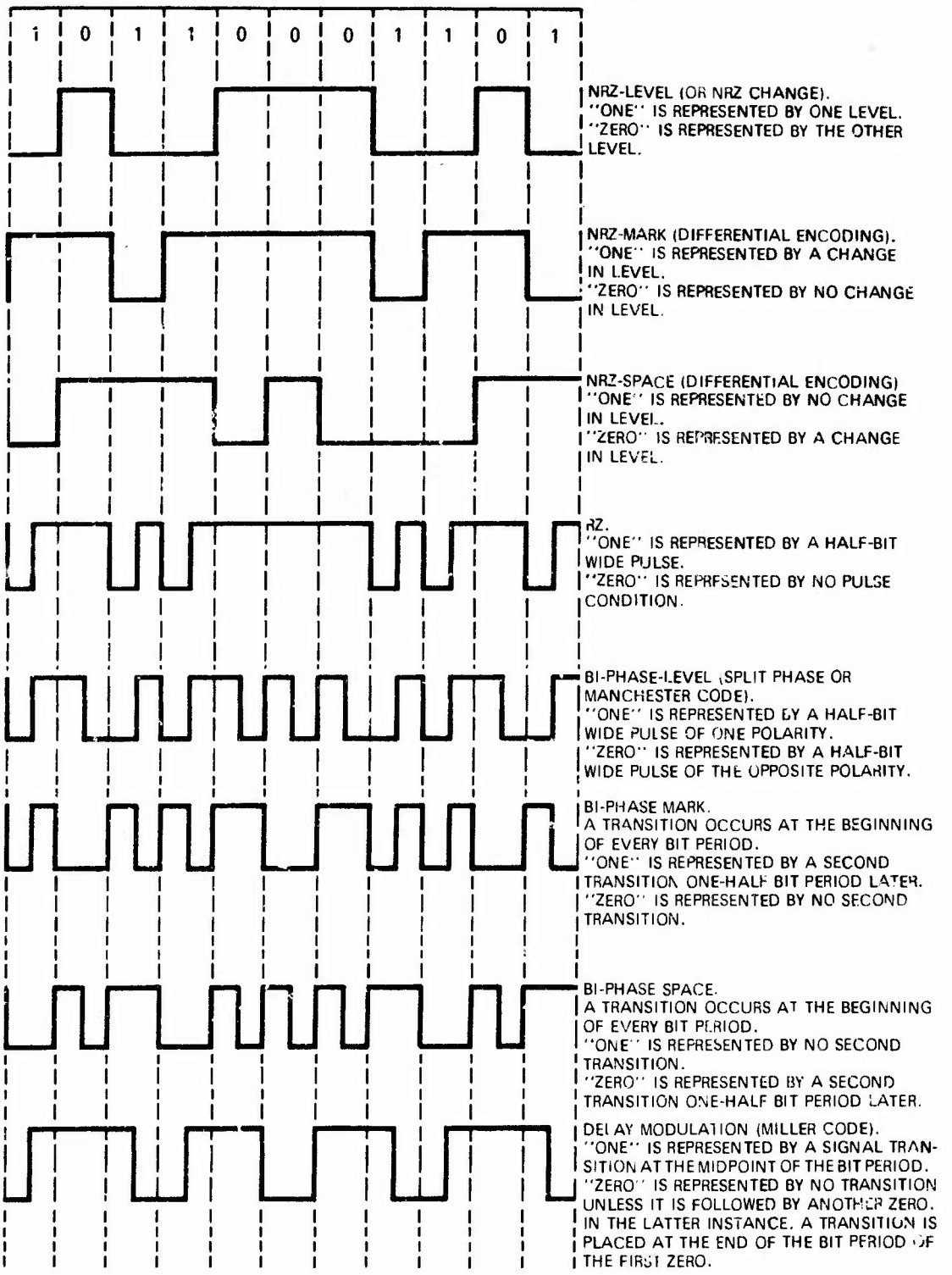

Figure 1-1. PCM Signaling Formats.

This optimum decision rule can be realized (see Fig. I-2) by constructing two cross-correlators and providing perfect bit synchronization to be used to sample the cross-correlator outputs. If the first cross-correlator output exceeds the second, we decide that $s_1(t)$ was present; otherwise, decide $s_2(t)$. Alternatively, the optimum decision circuit could be realized by constructing two matched filters having impulse responses $s_1(T-t)$ and $s_2(T-t)$; however, we do not pursue this realization since one generally implements Fig. I-2 in practice.

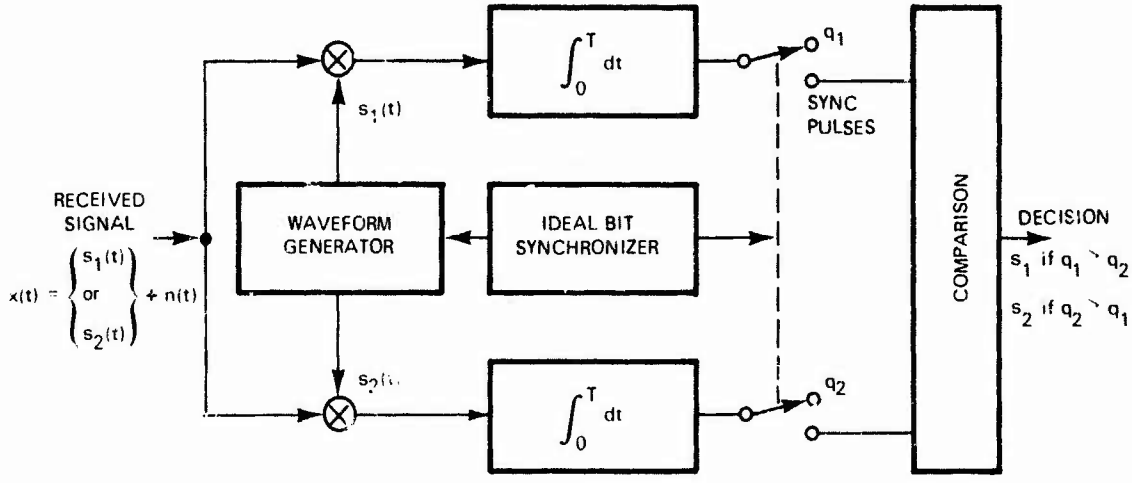

Figure I-2. Optimum Decision Circuit Assuming Perfect Bit Sync.

I-1. Theoretical Performance of Perfectly Synchronized PCM Signal Conditioners. The measure of system performance is bit error rate (BER). This measure of performance represents the average number of times an incorrect bit state occurs in a given time period. Frequently, the BER is expressed as the bit error probability (BEP) which is the ratio of the number of bits in error to a given number of bits transmitted.

In what follows we shall denote the BEP by the symbol P_E. For the case of perfect bit synchronization the BEP turns out to be a function of the ratio of the signal energy per bit, $E = ST$, to single-sided noise spectral density $N_0 = kT^0$ watts/Hz.[1] This ratio, say $R = E/N_0 = ST/N_0$, will be referred to as the signal energy-to-noise ratio per bit or more simple the signal-to-noise ratio (SNR). We now present the theoretical performance limitations for various PCM signal conditioners relating BEP to the signal-to-noise ratio $R = E/N_0 = ST/N_0$.

(a) The RZ Signaling Format. In what follows we shall summarize the performance of two types of RZ signaling. In both cases the signals s_1 and s_2 are selected such that they are orthogonal, i.e.,

$$\int_0^T s_1(t)s_2(t)dt = 0 \tag{I-4}$$

Type I-RZ signals are represented by

$$s_1(t) = \sqrt{S} \quad 0 \le t \le T$$

$$s_2(t) = 0 \quad 0 \le t \le T \tag{I-5}$$

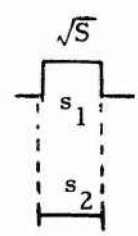

The BEP for Type I - RZ signaling is easily shown to be given by

$$P_E = \tfrac{1}{2}\,\mathrm{erfc}(\sqrt{R/4}) \tag{I-6}$$

[1] The thermal noise power generated per unit bandwidth is $\overline{v^2} = 4kT^oR$. When this source is matched to an ideal load of R ohms the noise power delivered is $\overline{v^2}/(R/2R)^2$.

where

$$\operatorname{erfc}(x) \triangleq \frac{2}{\sqrt{\pi}} \int_x^\infty e^{-t^2} dt \qquad \text{(I-7)}$$

This assumes that a threshold is established in the data detector at one-half the signal energy. If $q_1 > ST/2$ then s_1 is announced; otherwise, a decision is made in favor of s_2. This threshold is optimal for correlation detection.

Type II - RZ signals are defined by

$$s_1(t) = \begin{cases} \sqrt{S} & 0 \le t \le T/2 \\ -\sqrt{S} & T/2 \le t \le T \end{cases} \qquad \text{(I-8)}$$

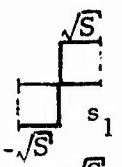

$$s_2(t) = \sqrt{S} \quad 0 \le t \le T$$

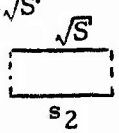

while the corresponding BEP is given by

$$P_E = \tfrac{1}{2} \operatorname{erfc}(\sqrt{R/2}) \qquad \text{(I-9)}$$

From (I-6) and (I-9) we conclude that RZ signaling of Type II is 3 dB superior to RZ signaling of Type I.

(b) <u>NRZ-L or Manchester (Split-Phase) Signaling</u>. NRZ-L signals are characterized as the negatives of each other, in fact,

$$s_1(t) = -s_2(t) \qquad 0 \le t \le T \qquad \text{(I-10)}$$

The BEP for a perfectly synchronized receiver is given by

$$P_E = \tfrac{1}{2} \operatorname{erfc}(\sqrt{R}) \qquad \text{(I-11)}$$

which says that the NRZ-L signaling format is 3dB superior to the Type II - RZ signaling format. This BEP can also be obtained with Manchester coding.

(c) NRZ-M and NRZ-S Signaling. NRZ-M and NRZ-S formats represent systems which employ differential encoding and differential decoding. For these cases the BEP can be shown to be given by

$$P_E = \tfrac{1}{2} \exp(-R) \qquad \text{(I-12)}$$

For R > 10 dB, NRZ-L and NRZ-M or NRZ-S yield approximately equivalent bit error probabilities.

(d) Miller Coding (Delay Modulation). To detect the Miller code a slightly different receiver mechanization of the data detector is required. If one examines only the data received during a single bit interval then the optimum data detector is illustrated in Fig. I-3. For convenience we

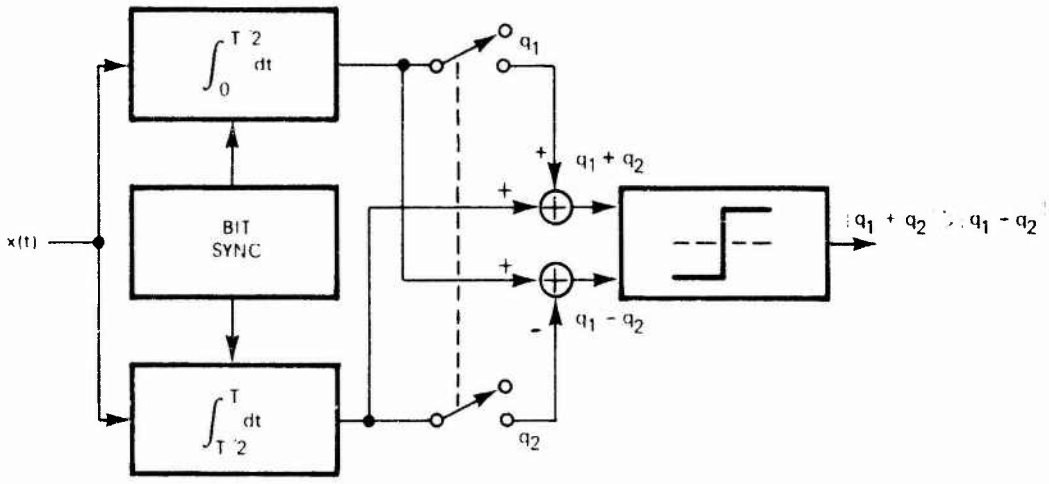

Figure I-3. Optimum Single-Shot Data Detector for the Miller Code.

assume that the transmitted signals are sequences of ±1's. For this case, the BEP is easily shown to be given by (Ref. 3)

$$P_E = \text{erfc}\left(\sqrt{\frac{R}{2}}\right)\left[1 - \tfrac{1}{2}\,\text{erfc}\left(\sqrt{\frac{R}{2}}\right)\right] \qquad \text{(I-13)}$$

For $R \gg 1$, we have from (I-13) that

$$P_E \approx \text{erfc}\sqrt{\frac{R}{2}} \qquad \text{(I-14)}$$

so that the BER is twice as large as that obtained with Type II - RZ signaling. If the performance of Miller codes is compared with NRZ-L (Manchester coding or split phase) then we see from (I-11) and (I-14) that the BEP for NRZ-L signaling is $\frac{1}{2}$ as large at 3 dB less signal-to-noise ratio as the BEP for Miller coding.

It is interesting to compare the performance of a Miller code with quadriphase, i.e., four phase PSK signaling. For quadriphase signaling it is easy to show that (Ref. 3)

$$P_E = \text{erfc}\sqrt{\frac{R}{2}}\left[1 - \tfrac{1}{4}\,\text{erfc}\sqrt{\frac{R}{2}}\right] \qquad \text{(I-15)}$$

$$\approx \text{erfc}\sqrt{R/2} \quad ; \quad R \gg 1$$

so that for $R \gg 1$ the BEP for quadriphase signaling is equivalent to the performance of the Miller code.

In passing we note that it appears possible to derive the optimum bit detectors for the Miller code when the infinite past and infinite future of the data are considered in the detection process. The BEP for the rather complicated data detectors has been evaluated and it

has been shown that such detectors perform superior to that of Fig. I-3 by less than 0.5 dB. The question as to whether one should mechanize the optimum data detector for Miller coding must therefore be determined by the complexity of data processing allowed in at the point of reception.

I-2. BEP Comparisons for the Case of Perfect Bit Synchronization. In summary we have that the BEP for RZ, NRZ and Miller code signaling is given by

$$\begin{aligned} BER_{RZ} &= \tfrac{1}{2}\,\mathrm{erfc}(\sqrt{R/4}) \quad ; \text{ Type I-RZ} \\ BER_{RZ} &= \tfrac{1}{2}\,\mathrm{erfc}(\sqrt{R/2}) \quad ; \text{ Type II-RZ} \\ BER_{\substack{\text{NRZ-L} \\ \text{Manchester}}} &= \tfrac{1}{2}\,\mathrm{erfc}(\sqrt{R}) \\ BER_{\text{Miller}} &= \mathrm{erfc}(\sqrt{R/2})\left[1 - \tfrac{1}{2}\,\mathrm{erfc}(\sqrt{R/2})\right] \end{aligned} \tag{I-17}$$

Fig. I-4 represents a plot of the BEP, as determined from these expressions, versus the signal-to-noise ratio $R = ST/N_0 = E/N_0$ in dB. Thus, using Miller coding, we see that for large R the BEP is approximately twice as large as can be obtained with NRZ-L with one half the power. For BEP's on the order of 10^{-3} or 10^{-5} Miller coding requires approximately 3.5 dB more power than NRZ-L or Manchester coding. On the other hand, Type II-RZ signaling is superior to Miller coding in this vicinity of BEP by approximately 0.5 dB while Type I-RZ is inferior to Miller coding by 2.5 dB.

Finally, for $R \gg 1$ or $P_E < 10^{-3}$ we note that

$$BER_{\text{Miller}} \approx BER_{\text{4-PSK}} \tag{I-18}$$

where the symbol 4-PSK implies quadriphase.

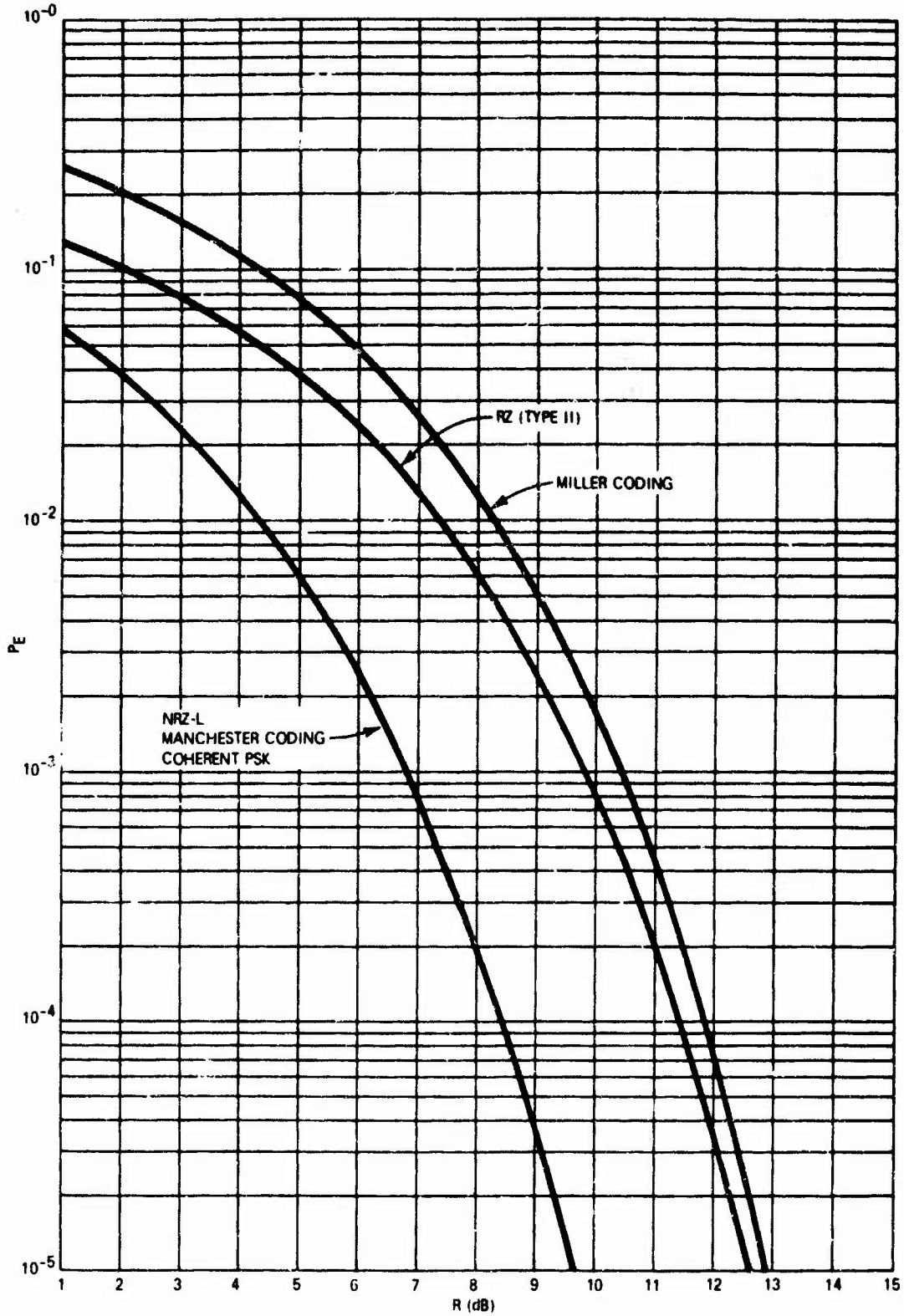

Figure I-4. BEP Versus R for Various Baseband PCM Signaling Techniques (Perfect Bit Sync Assumed).

II. SPECTRAL OCCUPANCY, BANDWIDTH CONSIDERATIONS AND THEIR EFFECTS ON BIT SYNCHRONIZATION (REFERENCE 3)

Aside from BEP considerations, a number of other factors must be taken into consideration when attempting to select a particular baseband signaling and bit synchronization technique. These include:

(1) Signal Bandwidth

(2) Signal Bit Synchronization Capabilities

(3) Signal Interference and Noise Immunity Properties

(4) Cost and Complexity of Implementation of the Data Detector and Bit Synchronizer

In what follows we discuss the spectral occupancy of the baseband signaling schemes by presenting the power spectral density functions and discuss their relationship to the problem of bit synchronization. We shall define

$$S_i(f) \triangleq \int_0^T s_i(t)\exp(-j2\pi ft)dt$$

to the Fourier transform of the elementary signal $s_i(t)$.

(a) Power Spectral Density for Type I-RZ Signaling. Here we have a situation where $S_2(f) = 0$ and

$$S_1(f) = \frac{T\sqrt{S}}{2}\left[\frac{\sin \pi fT/2}{\pi fT/2}\right]\exp(-j\pi fT/2) \qquad \text{(II-1)}$$

For a purely random, equal probable, source the power spectrum is given by

$$\left.\frac{S(f)}{E}\right|_{RZ} = \frac{\delta(f)}{16T} + \frac{1}{16T}\sum_{n=-\infty}^{\infty}\left(\frac{2}{n\pi}\right)^2\delta\left(f - \frac{n}{T}\right) + \frac{1}{16}\left(\frac{\sin \pi fT/2}{\pi fT/2}\right)^2 \qquad \text{(II-2)}$$

Notice the delta function, $\delta(f)$, appearing in the spectrum. The spike at $f = 1/T$ can be used to establish bit synchronization; however, the signal energy at $f = 1/T$ would produce a self-jamming effect on the establishment of bit sync.

(b) Power Spectral Density for NRZ-L Signaling. For NRZ signals defined by (I-10) with $s_1(t) = \sqrt{S}$ for $0 \leq t \leq T$ then the power spectral density is given by

$$\left.\frac{S(f)}{E}\right|_{NRZ-L} = \left(\frac{\sin(\pi fT)}{(\pi fT)}\right)^2 \qquad \text{(II-3)}$$

Notice that there exists no spikes in the spectrum and that $S(0) = E$. These facts are of considerable importance when the bit synchronization problem is considered.

(c) Power Spectral Density for Manchester Coding (Split Phase). In this case it is easy to show that

$$\left.\frac{S(f)}{E}\right|_{Manchester} = \frac{\left[\sin(\pi fT/2)\right]^4}{\left[\pi fT/2\right]^2} \qquad \text{(II-4)}$$

Notice here that the spectrum contains no delta functions; however, $S(0) = 0$. In contrast to RZ signaling, these facts make Manchester coding attractive from the viewpoint of obtaining bit synchronization from the received signal.

(d) Power Spectral Density for Miller Coding. For Miller coding the power spectral density can be shown to be given by (Ref. 1)

$$\left.\frac{S(f)}{E}\right|_{\text{Miller}} = \frac{1}{2x^2[17 + 8\cos 8x]} \cdot [23 - 2\cos x - 22\cos 2x - 12\cos 3x + 5\cos 4x + 12\cos 5x + 2\cos 6x - 8\cos 7x + 2\cos 8x] \qquad \text{(II-5)}$$

where $x = \pi fT$. Notice here that $S(0) = 0.1$ and that the spectrum contain no spikes. These spectral features make Miller coding attractive from the bit synchronization point of view.

(e) Spectral Comparisons for RZ, NRZ, and Miller Coding. Plotted in Fig. II-1 are the power spectral densities of RZ, NRZ, Manchester coding and Miller coding. The spectral properties of Miller coding which make it attractive for magnetic tape recording (as well as phase-shift keyed signaling) include:

(1) The majority of the signaling energy lies in frequencies less than one half the bit rate $\mathcal{R} = 1/T$.

(2) The spectrum is small at f = 0. This spectral minimum facilitates the problem of bit synchronization.

(3) A reduced spectral density in the vicinity of f = 0 is important in tape recording because of their poor d-c response.

(4) As a result of (3) a lower magnetic tape recording speed (higher packing density can be used).

(5) The Miller code is insensitive to the 180° phase ambiguity that is common to NRZ-L and Manchester coding.

(6) The bandwidth required for Miller coding is approximately $\frac{1}{2}$ that required by NRZ-L and $\frac{1}{4}$ that required for Manchester coding, see Fig. II-1.

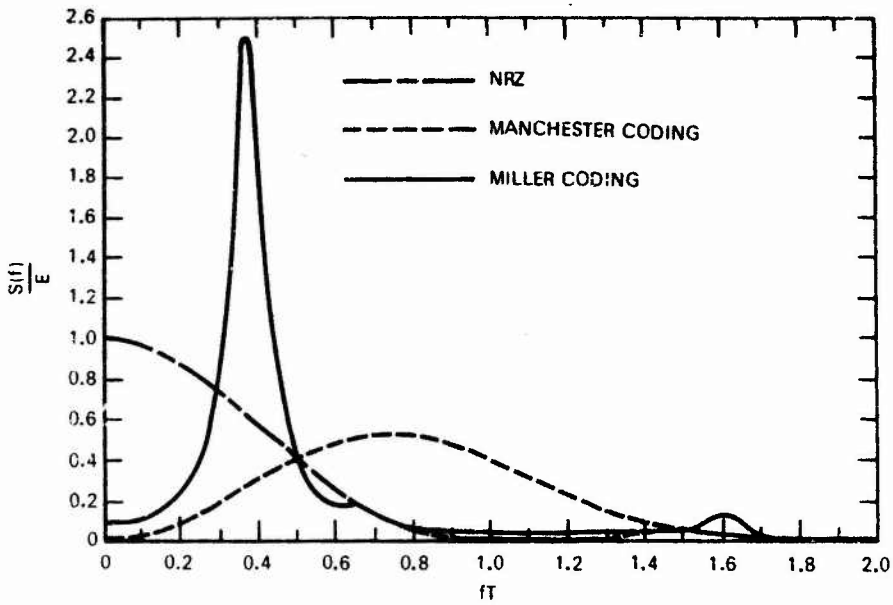

Figure II-1. Spectral Density of Random NRZ, Manchester Coding, and Miller Coding.

III. PERFORMANCE OF PCM SIGNAL CONDITIONERS IN THE PRESENCE OF BIT SYNC JITTER (REFERENCE 3)

In this section of the report we consider the combined problem of data (bit) detection and the effects of bit sync jitter on BEP. Our method of approach is to evaluate the BEP conditioned upon the fact that the bit synchronizer under consideration produces sync pulses, i.e., samples the output of the data detector, which are in error by τ second. Such a BEP will be called the conditional bit error probability (CBEP). We shall denote the CBEP by $P_E(\tau)$. This approach has the advantage that one can consider the effects of bit sync jitter on BEP for a broad class of bit

synchronization systems without having to specify the BEP for each situation. The average BEP is then obtained by averag ng the CBEP over the probability density function $p(\tau)$ of the bit sync jitter. The probability density function $p(\tau)$ is determined by the particular bit synchronization system under consideration. Thus, in general, we have that the average BEP is given by

$$P_E = \int_\tau p(\tau) P_E(\tau) d\tau \qquad \text{(III-1)}$$

We now present the conditional BEP expressions for RZ, NRZ, Manchester and Miller coding.

(a) Conditional BEP for Type I - RZ Signaling. If one establishes a threshold at $ST/2$ in the data detector and assumes that the bit sync sampling pulses are in error by τ seconds then the conditional BEP is easily shown to be given by (Ref. 3)

$$P_E(\tau) = \frac{1}{4}\left\{\text{erfc}\left(\sqrt{\frac{R}{4}}\right) + \text{erfc}\left[\sqrt{\frac{R}{4}}\left(1 - \frac{2|\tau|}{T}\right)\right]\right\} \qquad \text{(III-2)}$$

This result assumes rectangular on-off pulses characterized by (I- 5). When $\tau = 0$ this result reduces to (I- 6) as it should.

(b) Conditional BEP for Type II - RZ Signaling. For this case the signal pulses are characterized by (I- 8) and by establishing the optimum data detection threshold of zero, the CBEP is easily shown to be given by (Ref. 3)

$$P_E(\lambda) = \frac{1}{4}\left\{\text{erfc}\left[\sqrt{\frac{R}{2}}\right] + \text{erfc}\left[\sqrt{\frac{R}{2}}\left(1 - \frac{4|\tau|}{T}\right)\right]\right\} \quad ; \quad |\lambda| \le \frac{1}{4} \qquad \text{(III-3)}$$

when the bit sync error is τ seconds. When $\tau = 0$ this result reduces to (I- 9) as it should.

(c) Conditional BEP for NRZ-L Signaling. The signal pulses are characterized by (I-10). For a τ second bit synchronization error the CBEP can be shown to be given by (Ref. 3)

$$P_E(\tau) = \frac{1}{4}\left\{\text{erfc}(\sqrt{R}) + \text{erfc}\left[\sqrt{R}\left(1 - \frac{2|\tau|}{T}\right)\right]\right\} \qquad \text{(III-4)}$$

Notice that when $\tau = 0$ this result reduces to (I-11) as it should.

(d) Conditional BEP for Manchester Coding. Since Manchester coding requires a transition during every bit interval the CBEP is slightly higher than that of NRZ-L. In fact, it is easy to show that (Ref. 3)

$$P_E(\tau) = \frac{1}{4}\left\{\text{erfc}\left[\sqrt{R}\left(1 - \frac{2|\tau|}{T}\right)\right] + \text{erfc}\left[\sqrt{R}\left(1 - \frac{4|\tau|}{T}\right)\right]\right\} \qquad \text{(III-5)}$$

when the bit sync pulse is in error by τ seconds.

(e) Conditional BER for Miller Coding. Evaluation of the CBEP for Miller coding is slightly more difficult than the other PCM baseband signaling techniques considered thus far. The approach to developing the theoretical expression for the CBEP is to consider the data stream as composed of signal vectors $s_1 = (1, 1)$, $s_2 = (-1, 1)$, $s_3 = (-1, -1)$ and $s_4(1, -1)$. The conditional BEP given that s_1 was transmitted is given by

$$P_E(\tau|s_1) = P_E(\tau|s_1, \text{ no transition})\Pr[\text{No transition}] + P_E(\tau|s_1, \text{ transition})\Pr[\text{transition}] = P_E(\tau|s_3) \qquad \text{(III-6)}$$

Now the joint probability density function of the correlator outputs of Fig. I-3 given that x_1 is received, no transition occurs and the bit sync sampling pulse is in error by τ seconds is given by

$$p(q_1, q_2 | s_1, \tau, NTr) = \frac{1}{2\pi} \exp\left[-\frac{(q_1 - \sqrt{R})^2}{2}\right] \exp\left[-\frac{(q_2 - \sqrt{R})^2}{2}\right] \tag{III-7}$$

and when a transition occurs we have

$$p(q_1, q_2 | s_1, \tau, Tr) = \frac{1}{2\pi} \exp\left[-\frac{(q_1 - \sqrt{R})^2}{2}\right] \exp\left[-\frac{(q_2 - \sqrt{R}\left(1 - \frac{4|\tau|}{T}\right)^2}{2}\right] \tag{III-8}$$

Using these p.d.f.'s we have

$$P_E(\tau | s_1) = \int_0^\infty \int_{-\infty}^\infty p(q_1, q_2 | s_1, \tau, NTr) dq_1 dq_2 + \int_0^\infty \int^\infty p(q_1, q_2 | s_1, \tau, Tr) dq_1 dq_2 \tag{III-9}$$

This can be reduced to

$$P_E(\tau | s_1) = P_E(\tau | s_3) = \tfrac{1}{2} \operatorname{erfc}\left(\sqrt{\frac{R}{2}}\right)\left[1 - \tfrac{1}{2} \operatorname{erfc}\left(\sqrt{\frac{R}{2}}\right)\right] \tag{III-10}$$

$$+ \tfrac{1}{2} \operatorname{erfc}\left[\sqrt{\frac{R}{2}}\left(1 - \frac{4|\tau|}{T}\right)\right]\left[1 - \tfrac{1}{2} \operatorname{erfc}\left(\sqrt{\frac{R}{2}}\right)\right]$$

If we transmit $s_2 = (-1, 1)$ then the conditional BEP can be written as

$$P_E(\tau | s_2) = P_E(\tau | s_4) = P_E(\tau | s_2, NTr) Pr(NTr | s_2) + P_E(\tau | s_2, Tr) Pr[Tr | s_2] \tag{III-11}$$

If we note that $Pr[Tr] = 0$ and that $P_E(\tau|s_2) = P_E(\tau|s_4)$ due to the fact that the Miller code is insensitive to the 180 degrees phase shift then we can write

$$P_E(\tau|s_2) = P_E(\tau|s_4) = P_E(\tau|s_2, NTr) \qquad \text{(III-12)}$$

This probability can be evaluated in terms of the integral

$$P_E(\tau|s_2) = 2\int_0^\infty\int_0^\infty p(q_1, q_2|\tau, s_2)dq_1 dq_2 \qquad \text{(III-13)}$$

where the joint p.d.f. $p(q_1, q_2|\tau, s_2)$ is characterized by

$$p(q_1, q_2|\tau, s_2) = \frac{1}{2\pi}\exp\left[-\frac{(q_1+b)^2}{2}\right]\exp\left[-\frac{(q_2-b)^2}{2}\right] \qquad \text{(III-14)}$$

Direct substitution and simplification leads to

$$P_E(\lambda) = \frac{1}{2} + \frac{3}{16}\,\mathrm{erf}^2(a) + \frac{1}{16}\,\mathrm{erf}^2\left(\sqrt{\frac{R}{2}}\right) -$$

$$\frac{3}{4\sqrt{\pi}}\int_0^{\sqrt{2}b}\exp[-(x-\sqrt{R})^2]\,\mathrm{erf}\,x\,dx -$$

$$\frac{3}{4\sqrt{\pi}}\int_0^{\sqrt{2}b}\exp[\{-(x-\sqrt{R}(1-4|\lambda|)\}^2]\,\mathrm{erf}\,x\,dx \qquad \text{(III-15)}$$

where

$$a = \sqrt{\frac{R}{2}}\,(1-4|\lambda|)\,; \qquad b = \sqrt{\frac{R}{2}}\,(1-2|\lambda|) \qquad \text{(III-16)}$$

If the bit sync error τ is zero, then the above result reduces to I-13 as it should.

III-1. Numerical Evaluation of the BEP

In order to numerically evaluate the average BEP, it is convenient to characterize the probability density function $p(\tau)$ of the bit sync jitter as a function of the normalized bit sync error

$$\lambda = \tau/T \tag{III-17}$$

We shall postulate a probability density function of the bit sync error in such a manner that the numerical results obtained are in terms of the rms normalized bit sync jitter σ_λ. This approach has the advantage that the set of curves obtained of somewhat universal in that the effects of bit sync jitter on BEP is a function of the rms bit sync jitter, say σ_λ, is clearly manifested. Obviously

$$\sigma_\tau = \sigma_\lambda T \tag{III-18}$$

We shall assume that the average clock frequency of the bit synchronizer is equal to that of the data stream. The uncertainty is due entirely to the bit sync jitter.

In terms of the normalized bit sync error $\lambda = \tau/T$ the average BEP can be written as

$$P_E = \int_\lambda P_E(\lambda)p(\lambda)d\lambda \tag{III-19}$$

where $p(\lambda)$ is the probability density function (p.d.f.) of the normalized error $\lambda = \tau/T$. This p.d.f. is conveniently characterized, in terms of σ_λ, by (Ref. 2)

$$p(\lambda) = \frac{\exp\left[\dfrac{\cos 2\pi\lambda}{(2\pi\sigma_\lambda)^2}\right]}{I_0\left[\left(\dfrac{1}{2\pi\sigma_\lambda}\right)^2\right]} \quad ; \quad |\lambda| \leq \tfrac{1}{2} \qquad \text{(III-20)}$$

when RZ and NRZ signaling is employed. Here $I_0(x)$ is the modified Bessel function of order zero and imaginary argument.

For PCM baseband signaling techniques which employ transitions in the middle of every bit interval then the p.d.f. of the normalized bit sync error is characterized by

$$p(\lambda) = \frac{2\exp\left[\dfrac{\cos(4\pi\lambda)}{(4\pi\sigma_\lambda)^2}\right]}{I_0\left[\dfrac{1}{(4\pi\sigma_\lambda)^2}\right]} \quad ; \quad |\lambda| \leq \tfrac{1}{4} \qquad \text{(III-21)}$$

Substitution of (III-20) or (III-21) into (III-19) with the appropriate expression for $P_E(\lambda)$ and performing numerical integration on a digital computer leads to the graphical results of Figs. III-1, III-2, III-3 and III-4 for BER vs. the signal-to-noise ratio $R = ST/N_0$ with the normalized bit sync rms jitter $\sigma_\lambda = \sigma_\tau/T$ as a parameter.

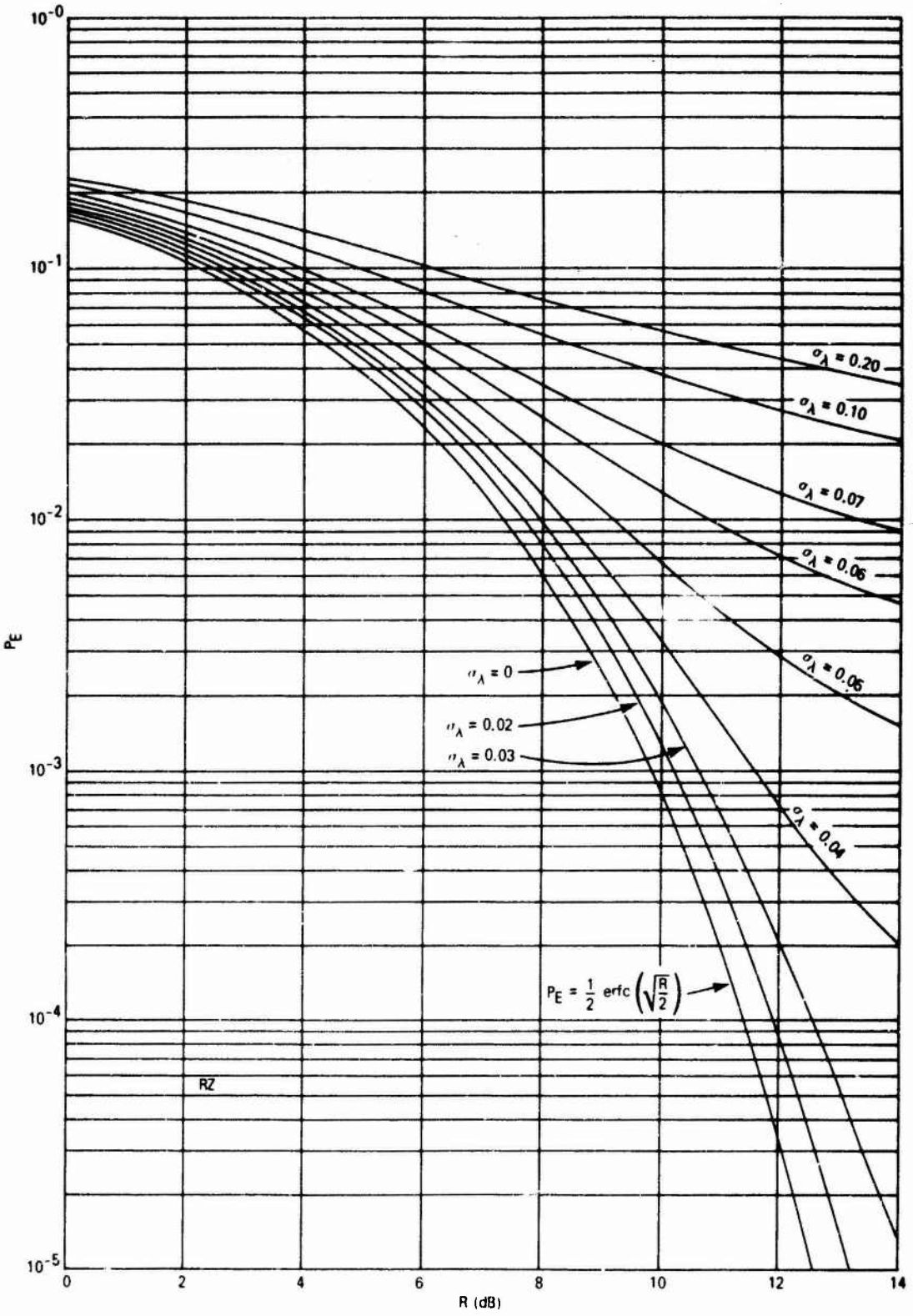

Figure III-1. BEP Versus R for Various $\sigma_\lambda = \sigma_\tau$ T (RZ).

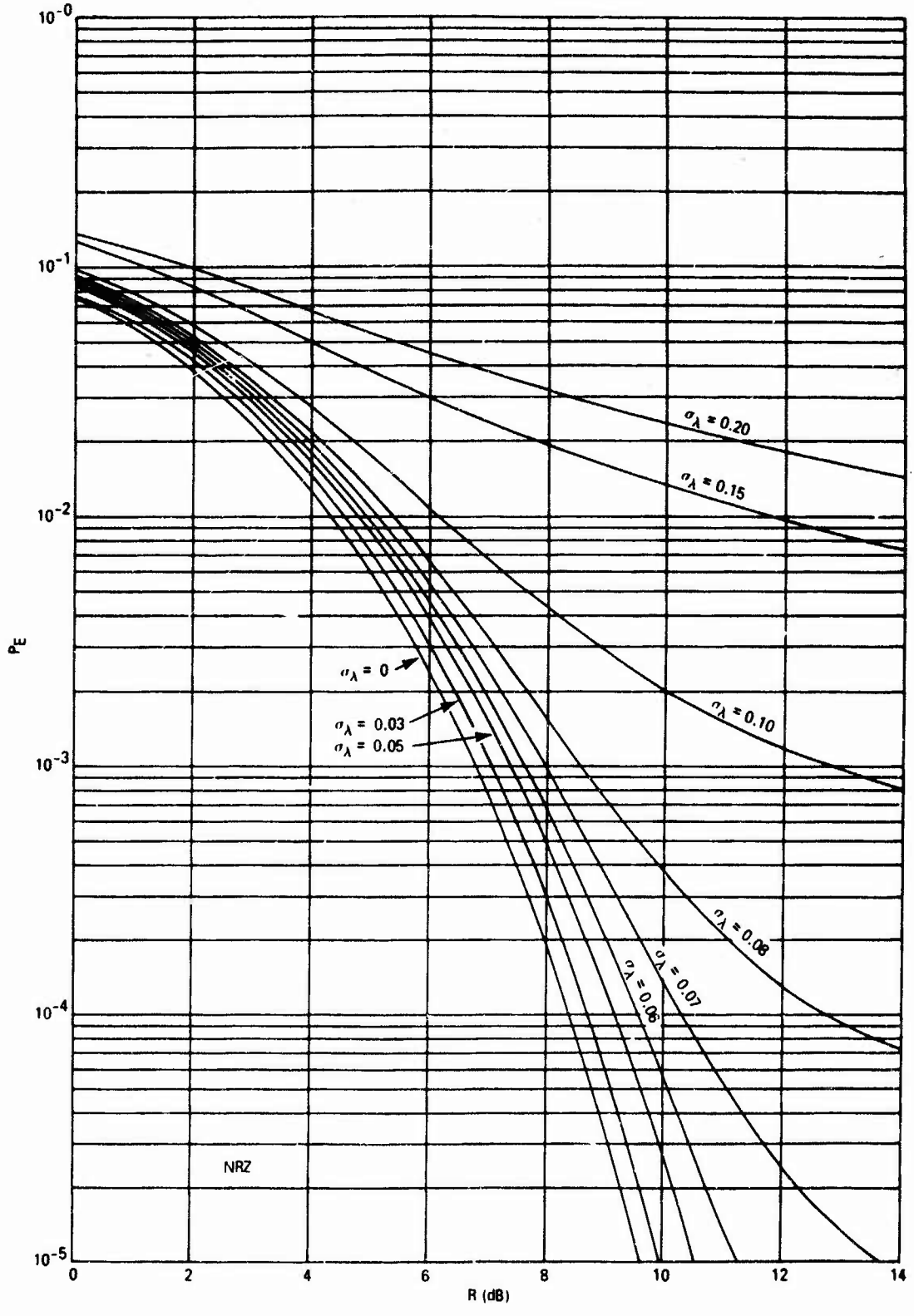

Figure III-2. BEP Versus R for Various σ_λ , σ_τ N (NRZ-L).

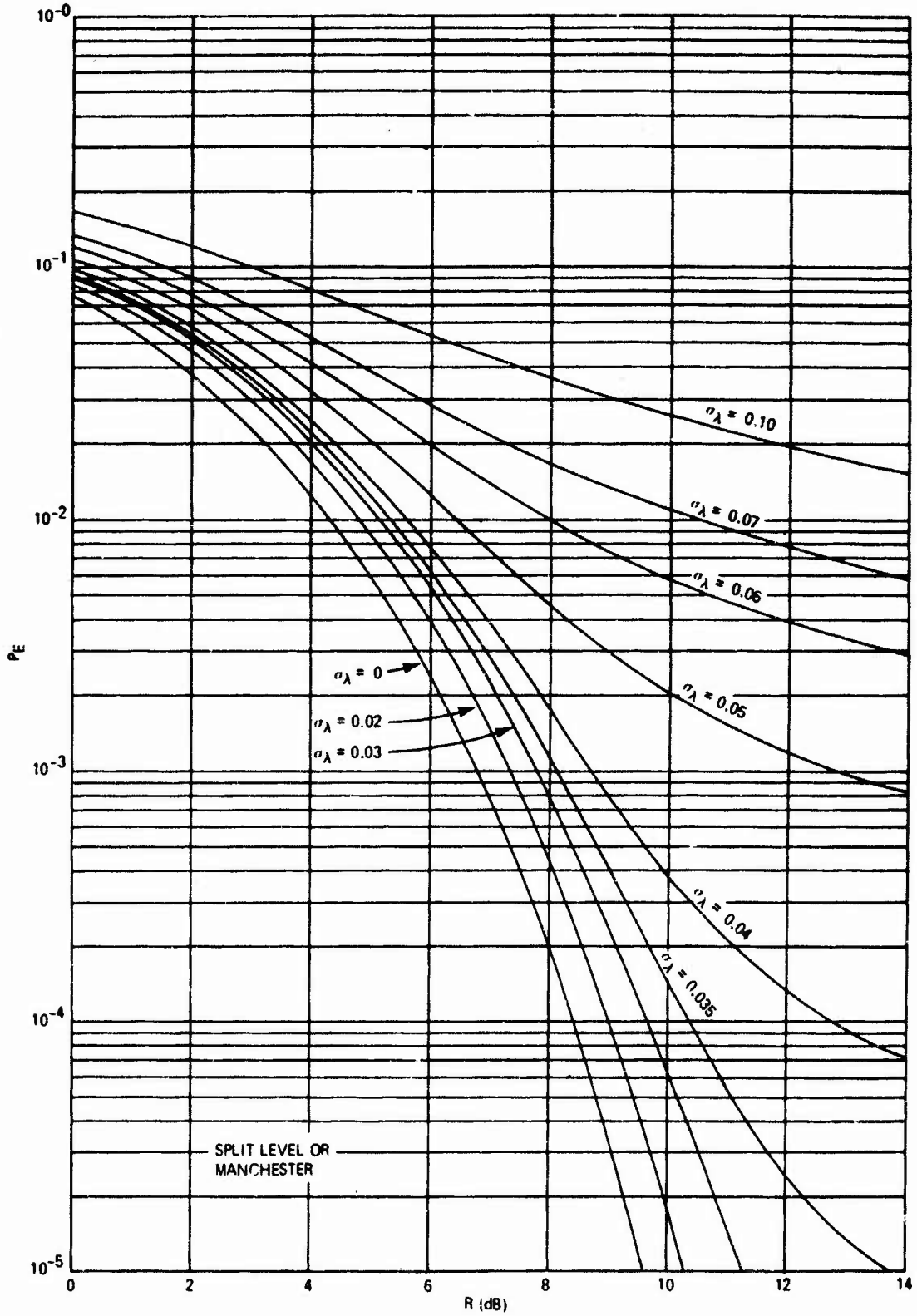

Figure III-3. BEP Versus R for Various $\sigma_\lambda = \sigma_\tau$ T (Manchester).

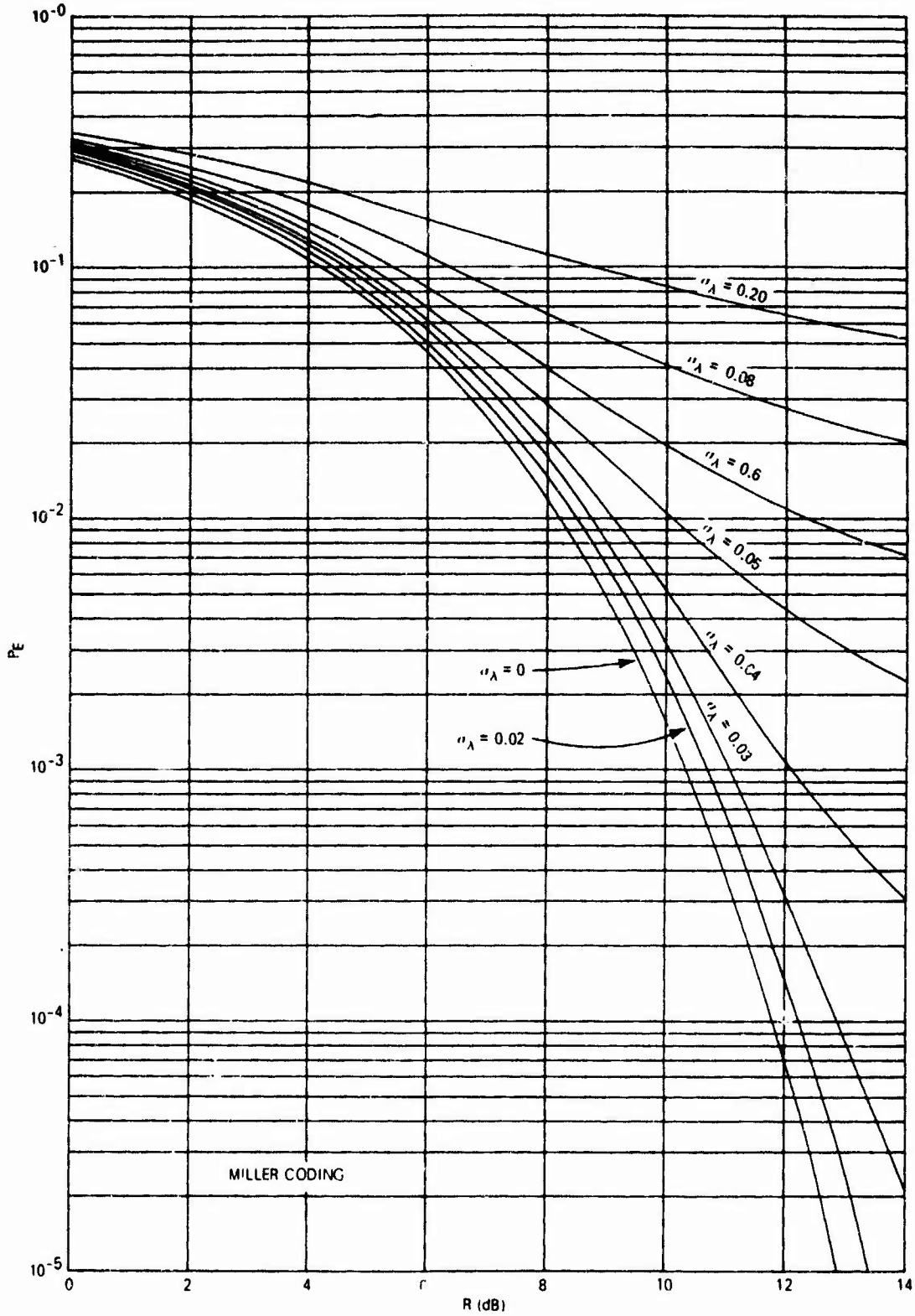

Figure III-4. BEP Versus R for Various $\sigma_\lambda = \sigma_\tau / T$ (Miller).

IV. BEP FOR NRZ-L SIGNALING WITH ARBITRARY WAVEFORMS

We now generalize the previous theory to include conditions where Gaussian noise is added to pulses of arbitrary shape. Such situations arise when the PCM data stream is filtered prior to detection. As before we consider the situation where the bit sync is in error by $\tau = \lambda T$ sec. The cross correlator output on which a decision is made for the n^{th} transmitted bit now depends on the received data in the time interval $(n-1)T + \hat{\epsilon} \leq t \leq nT + \hat{\epsilon}$ where $\hat{\epsilon}$ is the bit timing estimate obtained for the bit synchronizer. Stated mathematically,

$$\hat{a}_n = \text{sgn} \left\{ \int_{(n-1)T+\hat{\epsilon}}^{nT+\hat{\epsilon}} x(t) p_s[t - (n-1)T - \hat{\epsilon}]dt \right\} = \text{sgn } Q \qquad (IV-1)$$

where $\hat{a}_n$ is the n^{th} detected bit and $p_s(t)$ is the basic pulse shape of the PCM signal. The received PCM data stream plus noise is characterized by

$$x(t) = \sum_{k=0}^{K} a_k p_s[t - (k-1)T - \epsilon] + n(t) \qquad (IV-2)$$

and $a_k = \pm 1$ during the k^{th} transmission interval. Here ϵ serves as the pulse epoch or initial phase and K represents the number of bit intervals that ϵ is considered to be constant. If this expression is substituted into the above expression for $\hat{a}_n$ then by breaking Q into the signal component Q_s and noise component Q_n then it is easy to show that (Ref. 3)

$$Q_s = a_{n-1} R_s[-T(1-\lambda)] + a_n R_s(\lambda T) + a_{n+1} R_s[T(1+\lambda)] \qquad (IV-3)$$

where $R_s(\tau)$ is the signal pulse autocorrelation function $R_s(\tau)$ defined by

$$R_s(\tau) = \int_0^{T-\tau} p_s(t'+\tau)p_s(t')dt' \qquad \text{(IV-4)}$$

With regard to the input bits affecting the calculation of Q_s, one of four situations can occur: either the n^{th} bit and its adjacent bit are alike or they are unalike (negative followed by positive, or vice versa). In fact, if $\lambda > 0$ then a_n and a_{n+1} effect the decision while if $\lambda < 0$ then a_n and a_{n-1} enter into the decision variable. Hence, the CBEP is given by (Ref. 3)

$$P_E(\lambda) = \sum_{k=1}^{2} \left[\Pr\{n^{th} \text{ and adjacent bits} = (-1)^k\}\Pr\{\text{error} \mid n^{th} \text{ bit} = (-1)^k\}\right.$$

$$+ \Pr\{n^{th} \text{ bit} = (-1)^k \text{ and adjacent bit} = (-1)^{k+1}\} \cdot \qquad \text{(IV-5)}$$

$$\left.\Pr\{\text{error} \mid n^{th} \text{ bit} = (-1)^k\}\right]$$

Since the random variable Q is conditionally Gaussian on a_{n-1}, a_n, a_{n+1} and $\tau = \lambda T$ fixed, the input bits occur with equal probability and are independent, and $\sigma_Q^2 = N_0E/2$, it is easy to show that (Ref. 3)

$$P_E(\tau) = \tfrac{1}{4}\,\mathrm{erfc}\{\sqrt{R}[r_s(\tau) + r_s(1 - |\tau|)]\}$$

$$+ \tfrac{1}{4}\,\mathrm{erfc}\{\sqrt{R}[r_s(\tau) - r_s(1 - |\tau|)]\} \qquad \text{(IV-6)}$$

where

$$r_s(\tau) \triangleq \frac{R_s(\tau)}{E}$$

The average BEP is found from (III-19) and (III-20) using this result.

In passing we note that for rectangular pulses

$$r_s(\tau) = \begin{cases} 1 - \frac{|\tau|}{T} & |\tau| \leq T \\ 0 & |\tau| \geq T \end{cases} \qquad \text{(IV-7)}$$

To obtain numerical results for various filtered PCM signals numerical integration is required.

V. BIT SYNCHRONIZATION SYSTEM PERFORMANCE MEASURES (REFERENCE 2)

In this section of this report we shall digress from the problem of bit detection and consider the companion problem of bit synchronization. The motivation here is very simple: There has been very little useable theory developed which allows one to determine the tradeoffs which can be realized in the design and operation of a bit synchronization system (BSS) during bit sync acquisition and bit sync tracking. This is particularly true when the input to the BSS is a PCM signal. The lack of concentration on formulating and characterizing the fundamental limitations of BSS has lead to difficulties in not only procuring BSS but also in implementing them such that accurate and predictable procurement specifications can be met. For example, builders of commercial bit synchronizers usually do not adequately specify or characterize the acquisition or tracking performance of a particular bit synchronizer. Certainly, the state of affairs is such that tradeoffs in the two modes (tracking and acquisition) cannot be satisfactorily made. For example, a BSS configuration is usually changed by varying the system "bandwidth" by means of a switch on the front panel. The primary reason for this situation is that the theory has not been

satisfactorily advanced oweing to the nonlinear nature of a multi-dimensional problem.

One purpose of this report is to discuss the many parameters which serve to characterize the performance of a BSS. This discussion is given so that people, who are responsible for procuring BSS, can become aware of what is required in writing a bit sync specification, what parameters are reasonable and meaningful to spec and what constitutes physically realizable specifications. Before attempting to set forth any theory it seems appropriate to discuss the many facets of the bit sync problem. This will set the tone for that which follows.

V-1. Operational Behavior and Performance Characterization of Bit Synchronizers. The operation of any bit synchronization system (BSS) is conveniently discussed by considering its two modes of operation, namely, the acquisition mode (achieves the synchronous state) and the synchronous or tracking mode (retains the synchronous state). On the other hand, the performance of any BSS is characterized by certain performance measures which are statistical in nature when noise is present and deterministic when noise is absent. In order to introduce these performance measures we shall discuss the operational behavior of BSS from the viewpoint of rotating phasors. This point of view has the distinct advantage of being simple without losing generality in illustrating the operational behavior of a BSS.

Let the real part of the phasors $\exp[i\Phi(t)]$ and $\exp[i\hat{\Phi}(t)]$ be associated with the signals $s(t, \Phi)$ and $r(t, \hat{\Phi})$, respectively. These phasors, which rotate with instantaneous angular velocities $\omega(t) \triangleq \dot{\Phi}(t)$ rad/sec and

$\hat{\omega}(t) \triangleq \dot{\hat{\Phi}}(t)$, respectively, are shown in Fig. V-1. The bit sync error, $\varphi(t) \triangleq \Phi(t) - \hat{\Phi}(t)$, has temporal characteristics which are strongly dependent on the application and mode of operation; however, the performance measures associated with the random process $\{\varphi(t)\}$ are essentially independent of the application. We note that when the phase function $\Phi(t)$ is characterized by a random process the signal phasor $\exp[i\Phi(t)]$ and reference phasor $\exp[i\hat{\Phi}(t)]$ rotate randomly at rates proportional to $\dot{\Phi}(t)$ and $\dot{\hat{\Phi}}(t)$.

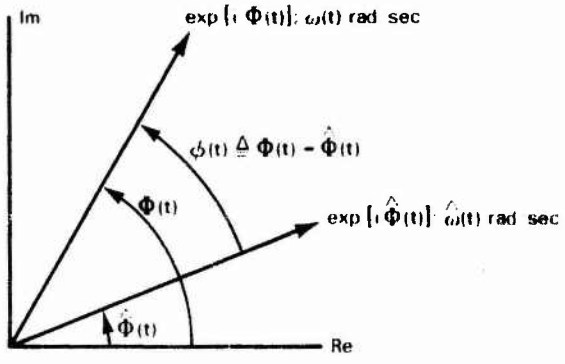

Figure V-1. Phasor Diagram for Describing Operation of a BSS.

(a) Acquisition Mode. Suppose the system enters the acquisition mode at $t = t_0$. Initially the phasors $\exp[i\Phi(t)]$ and $\exp[i\hat{\Phi}(t)]$ rotate at angular velocities $\omega \triangleq \omega(t_0)$ and $\omega_0 = \hat{\omega}(t_0)$ rad/sec respectively. Thus, initially $\exp[i\Phi(t)]$ rotates at rate $\Omega_0 \triangleq \dot{\varphi}(t_0) = \dot{\varphi}_0 = \omega - \omega_0$ rad/sec relative to $\exp[i\hat{\Phi}(t)]$. The parameter $\Omega_0/2\pi$ is called the initial frequency detuning in the system.

Figure V-2 shows a typical behavior of $\varphi(t)$ and $\dot{\varphi}(t)$ for a second-order BSC operating in the acquisition mode without an acquisition aid in the absence of noise. From this figure it is clear that the behavior of $\varphi(t)$ and $\dot{\varphi}(t)$ during acquisition is highly dependent upon the initial state

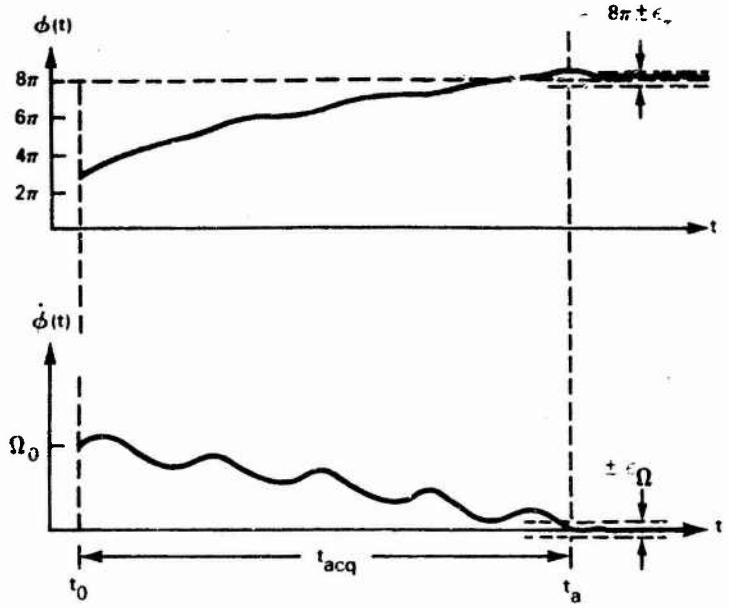

Figure V-2. Typical Behavior of ϕ and $\dot{\phi}$ for a BSS in the Acquisition Mode (Noise Absent).

$\underline{y}_0 \triangleq [\varphi(t_0), \dot{\varphi}(t_0)] = [\varphi_0, \dot{\varphi}_0]$. Let the synchronous mode be defined by the conditions $|\dot{\varphi}(t)| \leq \epsilon_\Omega$, $|\varphi(t) - 2n\pi| \leq \epsilon_\tau$, n any integer, for $t = t_a$. Suppose these conditions are satisfied at $t_{acq} = t_a - t_0$ for the first time. The parameter t_{acq} is called the signal acquisition time (often called pull-in time or lock-in time) since it is the time required to reach the synchronous mode. When noise is present the situation is much more complicated and we do not discuss all the details here; however, for this case t_{acq} become a random variable. Thus an important performance measure for the acquisition mode is the statistical moments $T^n_{acq} = E(t^n_{acq})$; $E(\cdot)$ denotes expectation in the statistical sense. Obviously, T^n_{acq} depends upon the initial state of the system. When the initial state is random and characterized by a probability density function (p.d.f.), then T^n_{acq} must be averaged over this density.

Shortly after acquisition, say $t > t_a$ seconds, the "steady-state" mean $\bar{\dot{\varphi}}/2\pi = (\omega - \bar{\omega}_V)/2\pi$ represents the mean residual frequency detuning. Here $\bar{\omega}_V$ is the average radian frequency of the synchronized generator and $(\omega_0 - \bar{\omega}_V)/2\pi$ is the mean frequency shift of the waveform generator to be synchronized. When $\dot{\Phi}(t) = \omega$ is constant, the largest value of Ω_0, say $|\Omega_0|_m$, from which the system can reach the synchronous mode is called the signal acquisition (often called pull-in or lock-in) range; that is, $|\Omega_0|_m$ represents the maximum relative angular velocity between phasors $\exp[i\Phi(t)]$ and $\exp[i\hat{\Phi}(t)]$ for which acquisition is possible. Since noise is present, characterization of the probability of acquisition at time t is also of interest.

In the acquisition mode, a BSS is highly nonlinear. In fact, the so-called linear theory cannot be used to carry out a particular design nor can it be used to account for the system's operational behavior; that is, the acquisition problem is characteristically nonlinear.

(b) Synchronous or Tracking Mode. Once the system is in the synchronous mode a more or less steady-state condition exists and the system tends to automatically make adjustments so as to maintain $|\varphi(t) - 2n\pi| \leq \epsilon$ and $|\dot{\varphi}(t)| \leq \epsilon_\Omega$ with high probability; that is, it tends to maintain the synchronous state. Due to the effects of noise, $n_i(t)$, and instabilities in the generator to be synchronized, random fluctuations in $\varphi(t)$ take place; see 3.

Figure V-3. Fluctuation of ϕ in the Synchronous Mode.

In the synchronous mode a number of performance measures are required to characterize and explain system behavior. The reason is that the performance measures which characterize this mode of operation are complicated to account for when both the system nonlinearity and noise are taken into consideration. If the system is linearized to simplify the problem, the performance measures which serve to characterize the fundamental behavior usually have no meaning; that is, operation in the synchronous mode is also characteristically nonlinear.

In this mode the time-dependent, conditional transition p.d.f. $P(\varphi, t | \underline{y}_0, t_0)$ of the absolute phase error $\varphi(t)$ is of interest. Furthermore, the reduced phase error $\varphi_r(t) \triangleq [\varphi(t) + \pi] \bmod 2\pi + (2n-1)\pi$ (such as displayed by a phase meter) is of interest. Here n is considered to be any fixed integer. See Fig. V-4 for a typical sample function of $\varphi_r(t)$ and $\varphi(t)$.) In loose terms, the bit sync error process $\{\varphi_r(t)\}$ is called the modulo-2π process. Thus the time-dependent, conditional transition p.d.f. $p(\varphi_r, t | \underline{y}_0, t_0, n)$ of the bit sync error, $\varphi_r(t)$, which a phase meter would read and the steady-state conditional transition p.d.f. $p(\varphi_r | n)$ are of importance.

With the passage of time, noise causes <u>bit slippage</u> to occur. Here we define bit slippage as the change of φ from φ_0 to $\varphi_0 + 2\pi$ or $\varphi_0 - 2\pi$, i.e., $\Delta\varphi/2\pi = \pm 1$ cycle; see Fig. V-4a. This corresponds to the situation in Fig. V-4 where, for any initial state $\underline{y}_0 = [\varphi_0, \dot{\varphi}_0]$, the phasor $\exp[i\Phi(t)]$ rotates $\pm 2\pi$ radians relative to the phasor $\exp[i\hat{\Phi}(t)]$. In physical terms the generator to be synchronized drops or adds one cycle of oscillation in $r(t, \hat{\Phi})$ relative to $s(t, \Phi)$; or stated another way, the signal $s(t, \Phi)$ is is shifted $\pm T$ seconds relative to the reference signal $r(t, \hat{\Phi})$. This phenomenon is called <u>bit slippage</u>.

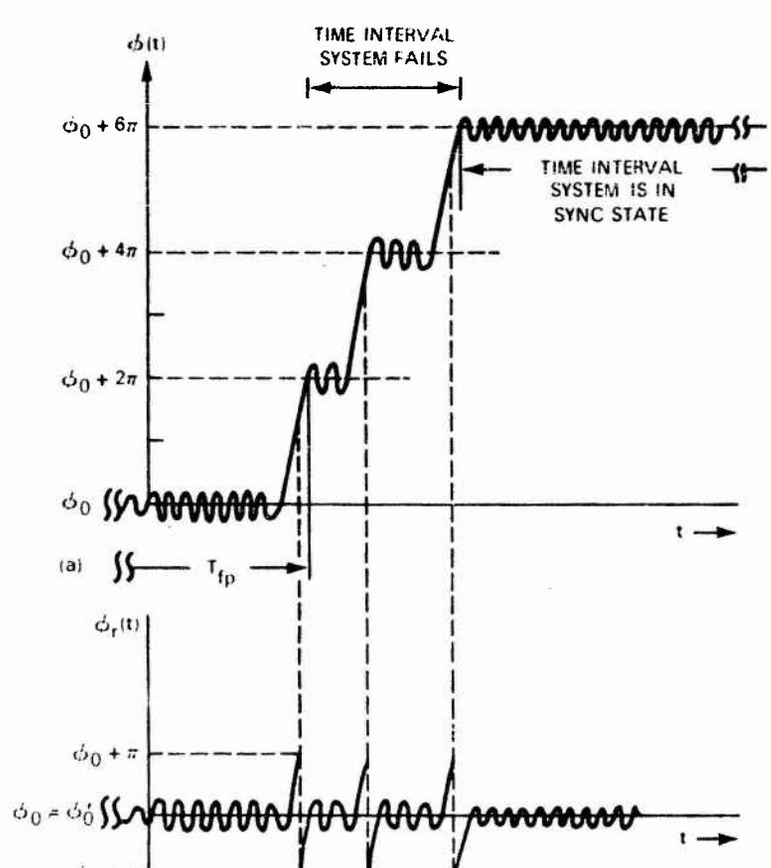

Figure V-4. Bit Slipping in BSS (a) Timing Error $\phi(t)$, (b) Reduced Timing Error $\phi_r(t)$. (Reference 2.)*

In the presence of noise and oscillator instabilities, bit slippage leads to frequency and phase diffusion in the generator to be synchronized. Therefore, the average bit slippage rate $\bar{S}$, is of interest. Since the time, T_{fp}, for bit slippage to occur for the first time is a random variable, see Fig. V-4a, we are interested in its statistical description by means of its p.d.f. or its moments, i.e., $E(T_{fp}^n)$. The first moment of this time is called the average time to first loss of bit sync and denoted by $E(T_{fp})$.

*William C. Lindsey, *Synchronization Systems in Communication and Control*, (c) 1972. Reprinted by permission of Prentice-Hall, Inc., Englewood Cliffs, New Jersey.

The probability of bit sync failure, P(t), in the time interval $[t_0, t]$ as well as the probability of slipping n bits, P(N=n), in the time interval $[t_0, t]$ are of interest. Since biases are frequently present in BSS, the average number of clockwise (counterclockwise) rotations per second of the phasor $\exp[i\Phi(t)]$ through 2π relative to the phasor $\exp[i\hat{\Phi}(t)]$ and the respective probabilities are of interest. We shall refer to the dropping and adding of oscillations in $r(t, \hat{\Phi})$ relative to $s(t, \Phi)$ as bit slippage to the right and left, respectively. The average number of bits slipped to the right (left) per second is characterized by N_+ (N_-). Other parameters which require a statistical characterization by means of the nonlinear theory include the average time, ΔT, between bit slipping events and the average time the BSS remains out of the synchronous state; see Fig. V-4a.

Table V-1 summarizes the measures of performance which serve to characterize the fundamental behavior of BSS systems. It is clear that the design or procurement engineer has a multitude to consider; however, in what follows we shall be primarily concerned with bit slippage rate, bit sync jitter, bit sync acquisition time and bit sync acquisition range. The bit error probability performance has been considered in an earlier part of this report. A rather complete bibliography of reference material is given in the list of references.

Table V-1. Performance Characterization of BSS (Reference 2)*

Acquisition Mode	Tracking Mode
1. Bit sync acquisition range	1. Steady state p.d.f. of bit sync
2. Bit sync acquisition time	2. Statistical moments of the bit sync
3. Probability of acquisition at time t	3. Moments of time to first loss of synchronization (sync)
4. Bit sync acquisition figure of merit	4. Average time to first loss of bit sync
5. Bit sync acquisition behavior	5. Average number of bits slipped per unit time
	6. Probability of synchronization failures as a function of time
	7. Average number of bits slipped to the right and to the left per unit time
	8. Probability of k slips in T seconds
	9. Average time between bit-slipping events
	10. Average time duration of failure events
	11. Mean and variance of the reference generator's frequency error
	12. Phase (frequency) error diffusion constant
	13. Signal hold-in range

VI. MODEL OF A CLASS OF PCM BIT SYNCHRONIZATION SYSTEMS

Bit synchronization has to do with determining the instants in time when the modulation may change states. One approach to providing this timing information is to utilize a separate communication channel solely for establishing bit sync. More efficiently, however, are the techniques whereby this level of timing information can be obtained directly from the received PCM data bearing signal. For this

*William C. Lindsey, *Synchronization Systems in Communication and Control*, (c) 1972. Reprinted by permission of Prentice-Hall, Inc., Englewood Cliffs, New Jersey.

case a broad class of bit synchronization systems, suggested by maximum a posteriori estimation techniques, can be represented by the diagram of Figure VI. Specific phase detector characteristics included are the early-late gate type, those which incorporate an absolute value approach, a difference of squares approach or a hybrid of these approaches, and the decision-directed type. We shall discuss these approaches later on in this section; however, before we get involved with detailed comparisons of BSS circuits it is appropriate to discuss the problem on the basis of presenting various theorteical results which are available in rather general terms.

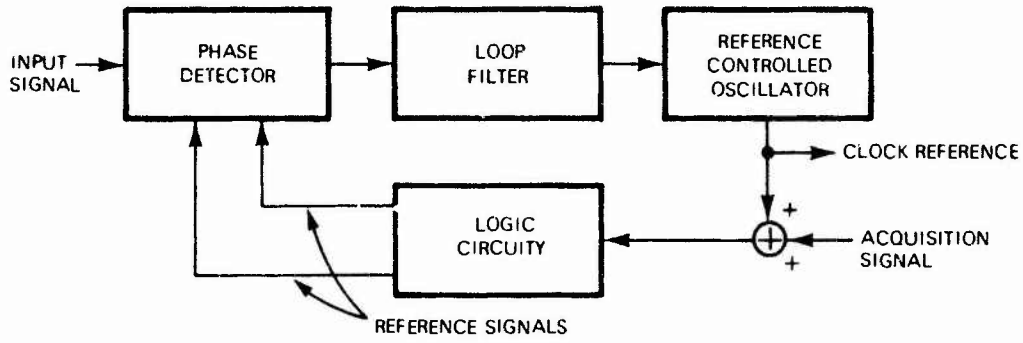

Figure VI. Model of a Class of Bit Synchronization Systems (BSS).

The math model for this class of BSS is illustrated in figure VI-1. Here $\tau(t)$ represent the time varying epoch to be tracked while $\hat{\tau}(t)$ represent the bit sync estimate and $\varphi(t) = \tau(t) - \hat{\tau}(t)$ represents the bit sync error. The phase detector characteristic $g(\varphi, t)$ is usually time-varying during the acquisition mode and can be considered to approach the steady state value $g(\varphi)$ when bit sync is achieved. The constant A represents the rms amplitude of the bit stream K is a gain determined by implementation and $n_g(t)$ is the equivalent additive noise

process which, in general, depends upon $g(\varphi, t)$. In fact, the stochastic, intergro-differential equation of operation is given by

$$\varphi = \tau(t) - \frac{KF(p)}{p}\left[Ag(\varphi,\ t) + n_g(t)\right]$$

where $p = d/dt$ denotes the linear operator which implies differentiation with respect to time. In fact, the above equation is a shorthand way of writing

$$\frac{d\varphi}{dt} = \frac{d\tau(t)}{dt} - AK\int_{-\infty}^{t} f(t-\lambda)\left[g(\varphi, \lambda) + n_g(\lambda)\right] d\lambda$$

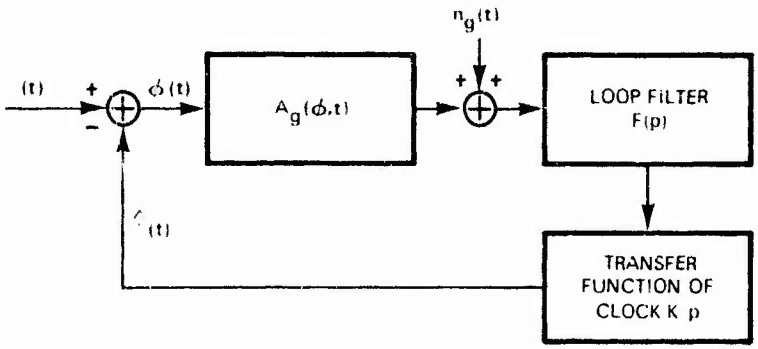

Figure VI-1. Math Model for a Broad Class of BSS.

VI-I. Acquisition Time and Acquisition Range For Two Different Phase Detector Characteristics

For the sake of definiteness we consider BSSs in which the loop filter assumes the form

$$F(s) = \frac{1 + \tau_2 s}{1 + \tau_1 s} = F_0 + \frac{1 - F_0}{1 + \tau_1 s} \qquad \text{(VI-1)}$$

where $F_0 = \tau_2/\tau_1$. Such a filter has the advantage of being capable of injecting a "quick reaction" type component of voltage directly into the

local clock generator to be synchronized as well as possessing (via a storing charge on a capacitor) memory. For this case a class of second-order BSS which employ the phase-lock principle are represented (in no noise) by the equation of operation

$$\frac{dx}{dt} = \Omega_0 - AKF_0[g(x)] + y_1$$
$$y_1 = -\left(\frac{1 - F_0}{1 + \tau_1 p}\right)[AK\, g(x)] \qquad \text{(VI-2)}$$

Here $\Delta f = \Omega_0/2\pi$ represents a frequency offset between the incoming and local clocks, g(x) represents the phase detector characteristic, AK represents the bit sync loop gain and x represents the instantaneous bit sync error. From this discussion we see that the acquisition time is a function of many variables including, in particular, the shape of the phase detector characteristic. For example, as we set

$$g(x) = \text{sgn}[\sin x] \qquad \text{(VI-3)}$$

then it can be shown (Ref. 2) that the time T_f required to eliminate bit slippage is approximated by

$$B_L T_f \approx \left[\frac{\frac{r+1}{8}\left[\frac{\pi^2}{4}\left(\frac{r+1}{r}\right)^2\left(\frac{\Delta f}{B_L}\right)^2\right]}{1 - \frac{F_0}{4 - F_0}\left[\frac{\pi(r+1)}{2r}\left(\frac{\Delta f}{B_L}\right)^2\right]}\right] \qquad \text{(VI-4)}$$

where $\Delta f = \Omega_0/2\pi$, B_L is the single side loop bandwidth, and $r = 4\zeta^2$ where ζ is the loop damping coefficient.

It is interesting to consider the case where the phase detector characteristic is sinusoidal, i.e., $g(x) = \sin x$. For this case it has been shown that (Ref. 3)

$$B_L T_f \approx \frac{\pi^2 (r+1)^3 \left(\frac{\Delta f}{B_L}\right)^2}{1 - \frac{F_0}{2-F_0}\left[\frac{\pi(r+1)}{2r}\left(\frac{\Delta f}{B_L}\right)^2\right]} \qquad \text{(VI-5)}$$

Comparing this result with that above, we see that the acquisition time for a sync system in which $g(x) = \text{sgn}[\sin x]$ is approximately 3dB faster than that of a sync system in which the phase detection characteristic is sinusoidal. Fig. VI-2 represents a plot of (VI-5) that is, the frequency acquisition time versus $|\Delta f|/B_L$ for a loop damping of 0.707 and various values of F_0.

The acquisition range $|\Delta f|_{max}$ is also interesting to compare as a function of the phase detector characteristic. In fact, for $g(x) = \text{sgn}[\sin x]$, it has been shown that

$$|\Delta f|_{max} < \frac{AK}{\pi}\sqrt{F_0(1 - F_0)} \qquad \text{(VI-6)}$$

while for a sinusoidal phase detector characteristic

$$|\Delta f|_{max} < \frac{AK}{2\pi}\sqrt{F_0(2 - F_0)} \qquad \text{(VI-7)}$$

Therefore, when $F_0 \ll 1$, the acquisition range for a rectangular phase detector characteristic is $\sqrt{2}$ times larger than for the sinusoidal phase detector characteristic.

Finally, it is interesting to compare the time to slip a cycle, say $T_{2\pi}$, near the boundary of synchronization for various phase detector

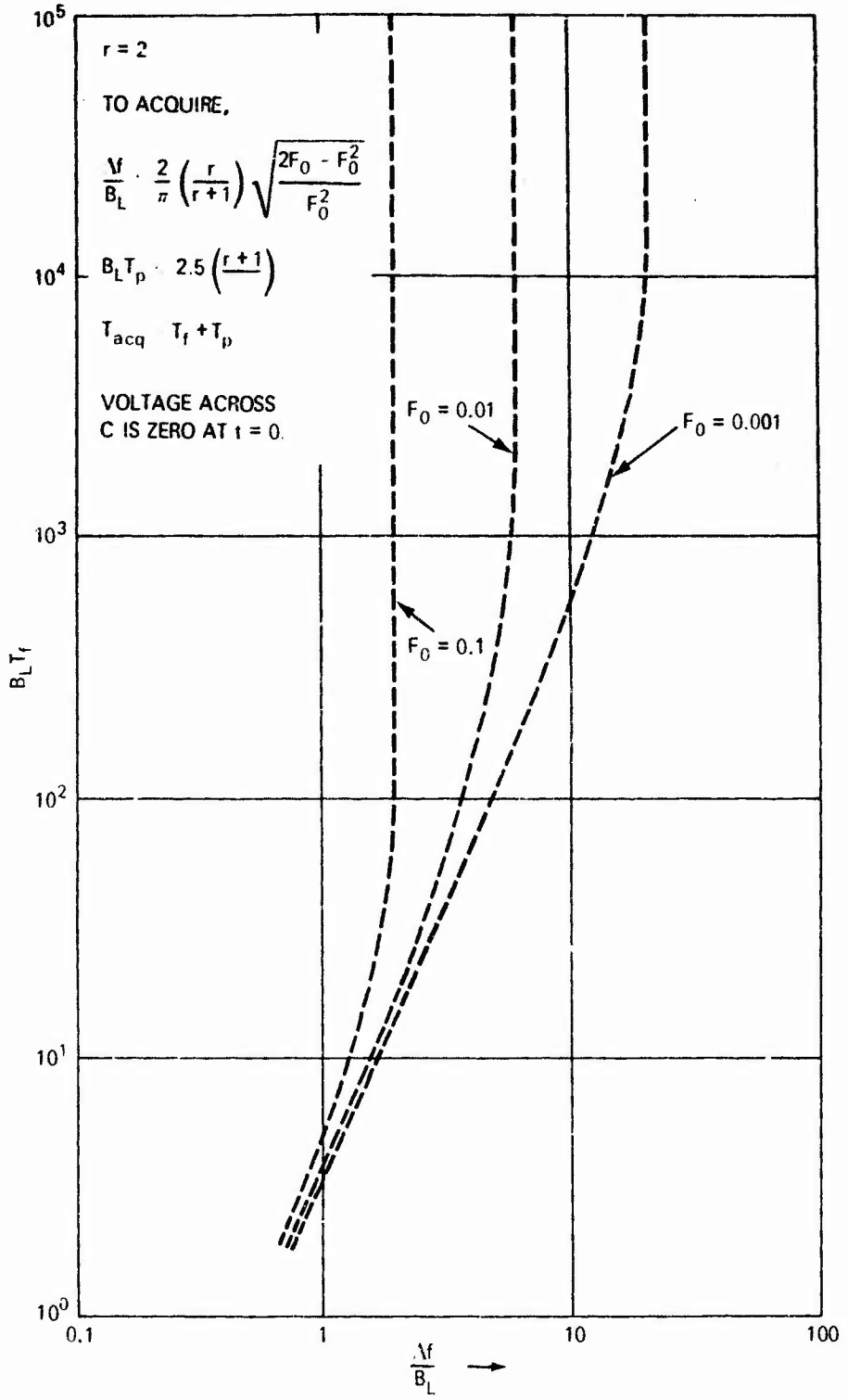

Figure VI-2. Acquisition Time Versus Normalized Frequency Offset for g(x) = sin x. (Reference 2.)*

*William C. Lindsey, *Synchronization Systems in Communication and Control*, (c) 1972. Reprinted by permission of Prentice-Hall, Inc., Englewood Cliffs, New Jersey.

characteristics. Since the derivation of such results are quite lengthy we merely present the results which were derived in (Ref. 2). There it is shown that the time to slip a cycle

$$T_{2\pi} \approx \begin{cases} \frac{2\pi}{AK}\sqrt{\frac{1}{F_0}} & ; \quad g(x) = \operatorname{sgn}[\sin x] \\ \frac{2\pi}{AK}\sqrt{\frac{2}{F_0}} & ; \quad g(x) = \sin x \\ \frac{2\pi}{AK}\sqrt{\frac{3}{F_0}} & ; \quad g(x) = \frac{\varphi}{\pi} \quad |\varphi| \leq \pi \end{cases} \tag{VI-8}$$

VI-2. Bit Slippage Rate as a Function of the Phase Detector Characteristic

The bit slippage rate, say $\bar{S}$, in a PCM bit synchronizer is an important parameter in that it gives a measure of the rate at which the bit sync reference fails. Although this parameter is difficult to account for in theory, it is instructive to present the theory to date for those cases for which it is analytically possible to evaluate.

If one considers the problem of obtaining the average number of bits slipped per second in a first-order BSS in which there exists zero frequency detuning and white noise present, then it is possible to show that the normalized slippage rate is given by (Ref. 2)

$$\frac{\bar{S}}{W_L} = \frac{(4/\alpha)}{\left[\int_{-\pi}^{\pi} \exp\left[\alpha \int^{\varphi} g(x)dx\right] d\varphi\right]\left[\int_{-\pi}^{\pi} \exp\left[-\alpha \int^{\varphi} g(x)\,dx\right] d\varphi\right]} \tag{VI-9}$$

where $\alpha = [1/2\pi k\sigma_\lambda]^2$ and $g(x)$ represents the phase detector characteristic. Here $\sigma_\lambda = \sigma_\tau/T$ represents the hit sync jitter and $k = 1$ for PCM signaling formats wherein no switching takes place in the middle of the bit interval

and k = 2 for PCM signaling techniques in which switching is possible in the middle of a bit interval.

For the case where there exists frequency offsets between the two clocks then it can be shown (Ref. 2) that

$$\frac{\bar{S}}{W_L} = \frac{4C_0'}{\alpha} \exp\left[-\frac{\gamma\alpha T}{2}\right] \cosh\left[\frac{\gamma\alpha T}{2}\right] \tag{VI-10}$$

where $\gamma = 2\pi\Delta f/AK$ and C_0' is a constant which normalizes the steady state probability density function of the bit sync jitter.

Let us now consider some special cases of the slip rate for two special phase detector characteristics. Consider first the phase detector represented by $g(x) = \text{sgn}[\sin x]$. For this phase detector characteristic it is easy to show that (Ref. 2)

$$\frac{\bar{S}}{W_L} = \frac{4}{\pi}\left[\frac{\exp(\pi\alpha) - 1}{\pi\alpha} - 1\right]^{-1} \tag{VI-11}$$

while for the sinusoidal phase detector characteristic

$$\frac{\bar{S}}{W_L} = \frac{1}{\pi^2\alpha I_0^2(\alpha)} \tag{VI-12}$$

Here $W_L = 2B_L$ represents the double sided loop bandwidth. Figures VI-3 and VI-4 represent the plot of $\bar{S}/2W_L$ for a sinusoidal phase detector characteristic and compares this with the $\bar{S}/W_L$ obtained for the rectangular phase detector characteristic $g(x) = \text{sgn}[\sin x]$. As before $\sigma_\lambda = \sigma_T/T$ represents the normalized bit sync jitter.

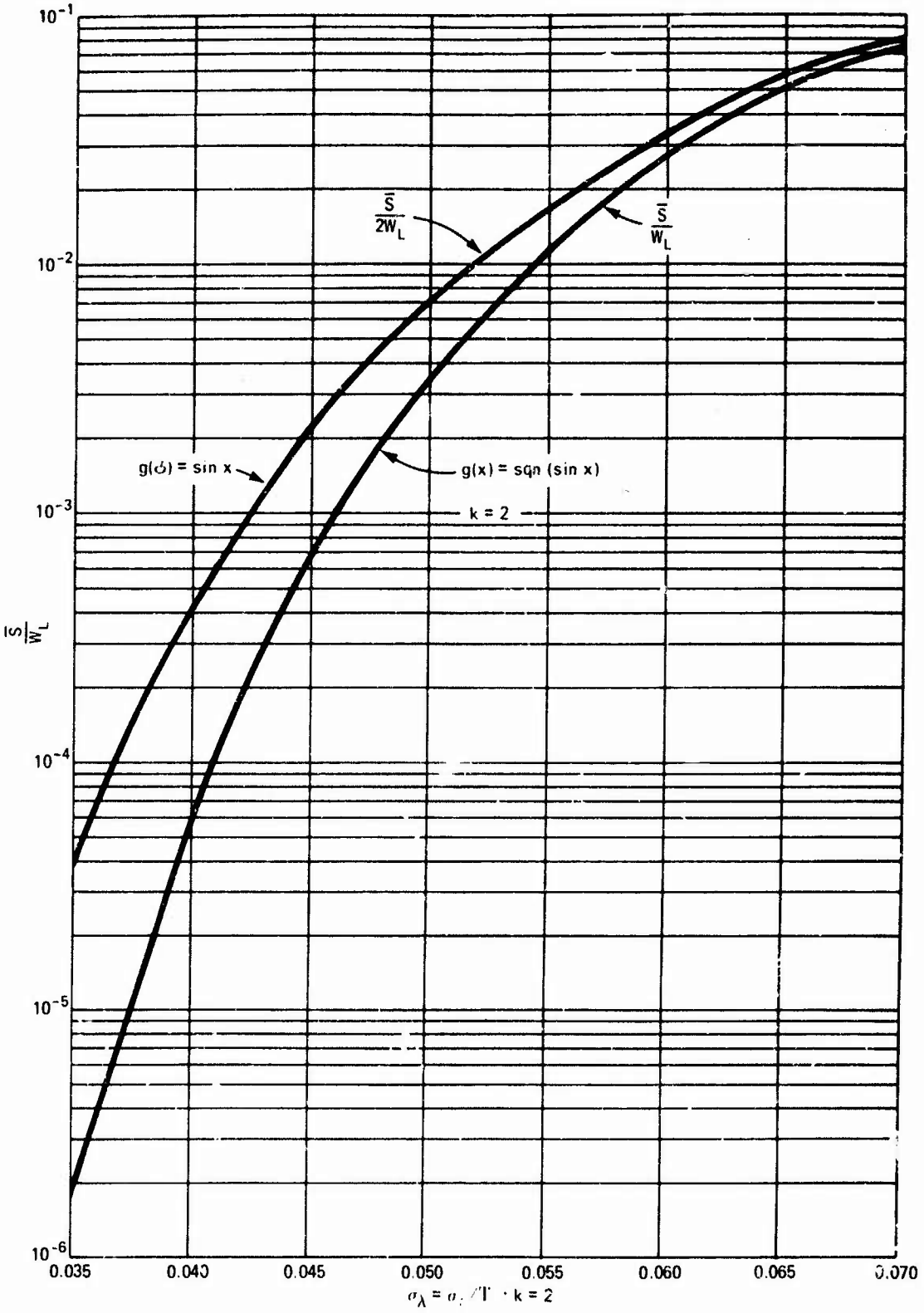

Figure VI-3. Bit Slippage Rate Versus Bit Sync Jitter.

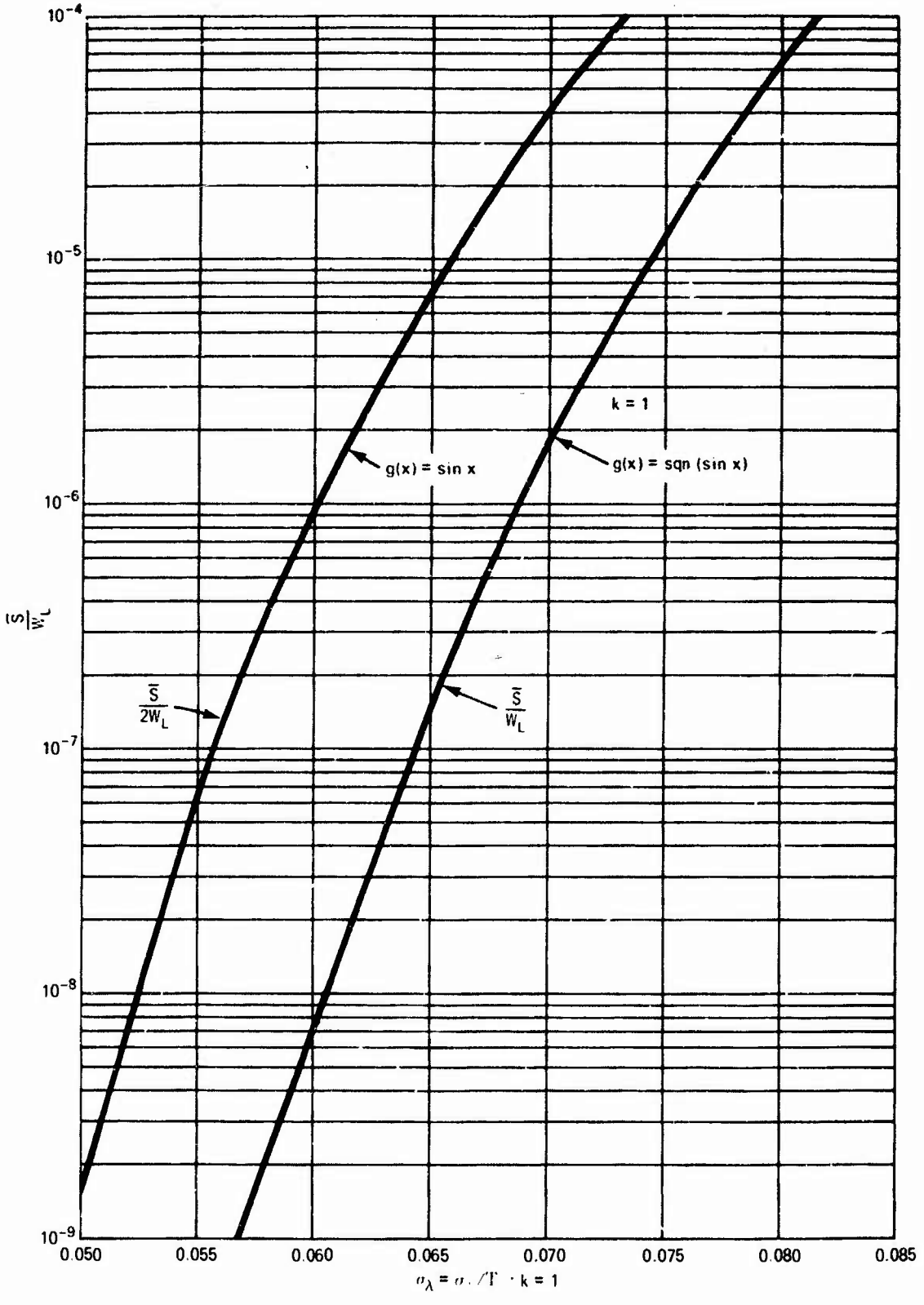

Figure VI-4. Bit Slippage Rate Versus Bit Sync Jitter.

VII. MATH MODELS AND THEIR RELATIONSHIP TO COMPUTER SOFTWARE

In order to develop a computer software program for a BSS one must determine several things. First of all, it is desirable to have a baseline BSS which is optimum. This is important because the performance measures which characterize its behavior serve as a limit beyond which no other BSS can outperform. The problem of selecting an optimum BSS for purposes of implementation or for carrying out performance comparisons largely remains an open question. For example, it is possible to use the techniques of maximum a posteriori (MAP) estimation and maximum likelihood estimation in order to specify an optimum bit sync circuit. Usually, owing to the nature of the statement of the problem, such a synchronizer turns out to be an open loop device. Furthermore, the criterion of selecting the peak of the a posterior probability density function or the likelihood function does in no way stress the importance of the acquisition problem. It should also be noted that the requirement of tracking bit sync, once it is obtained, places even stronger requirements on the MAP or maximum likelihood estimate. To force this requirement on the MAP estimator frequently leads one to a solution in which the MAP estimator is physically unrealizable; however, the open loop estimate can be used in a feedback loop to form a control loop which will track bit sync; however, the resulting close loop synchronizer which is suggested by the MAP estimator is suboptimum. These approaches have been the subject of much analytical and experimental investigation (see list of References).

For a maximum likelihood synchronizer Wintz and Luecke (Ref. 5) evaluate the mean magnitude bit sync error λ as a function of the PCM signal shape and a parameter, say T_m, which serves as an estimate of the number of bit durations that bit sync remains constant.

Quantitatively, the mean magnitude bit sync error varies inversely as the square root of T_m and $R = ST/N_0$, i.e.,

$$E|\lambda| \sim \frac{1}{T_m R}$$

The results of Monte Carlo computer simulation of performance are illustrated in Figs. VII-1 and VII-2.

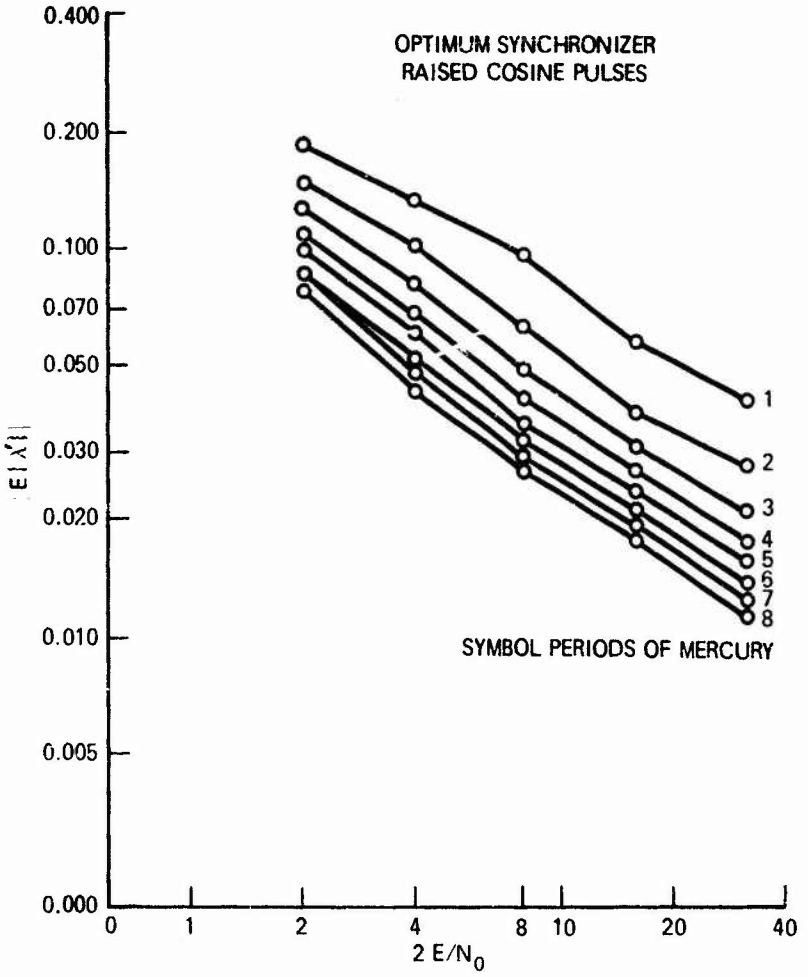

Figure VII-1. Mean Magnitude Bit Sync Error Performance of the MAP Synchronizer as a Function of Memory Time (Raised Cosine Pulses Assumed). (References 12, 13, 15, 18.)*

*Reprinted by permission of the Institute of Electrical and Electronics Engineers, Inc., 345 East 47th Street, New York, N.Y.

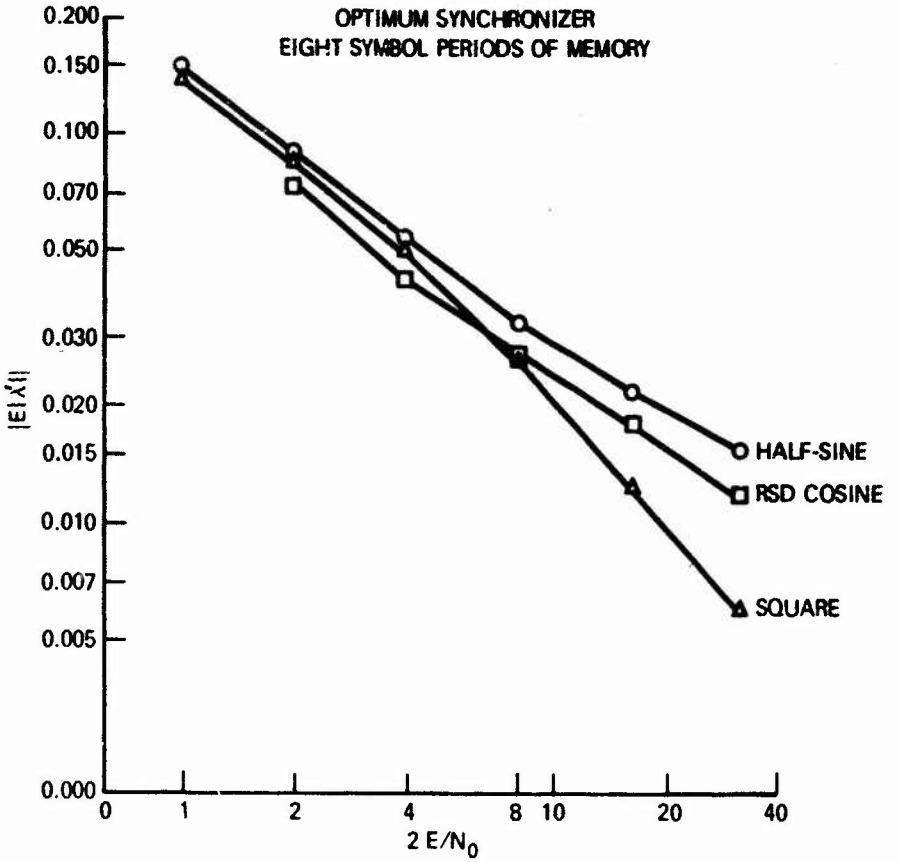

Figure VII-2. Mean Magnitude Bit Sync Error Performance of the MAP Synchronizer for Three Different Pulse Shapes and a Memory Time of Eight Symbol Periods. (Reference 5.)*

Other BSS suggested by closing the loop using a MAP estimator are suggested in Figs. VII-3 to 5. On the other hand, the digital data transition tracking loop (DTTL) of Fig. VII-6 represents a BSS which employs decision feedback and an error channel in which a "window" can be used to improve tracking performance. The parameter is used to adjust the window width. An early-late gate symbol synchronizer, its associated hit detector, and three different phase detector topologies are illustrated in Fig. VII-7 and 8. Finally, an absolute value type of BSS, say AVTS, is illustrated in Fig. VII-9.

*Reprinted by permission of the Institute of Electrical and Electronics Engineers, Inc., 345 East 47th Street, New York, N.Y.

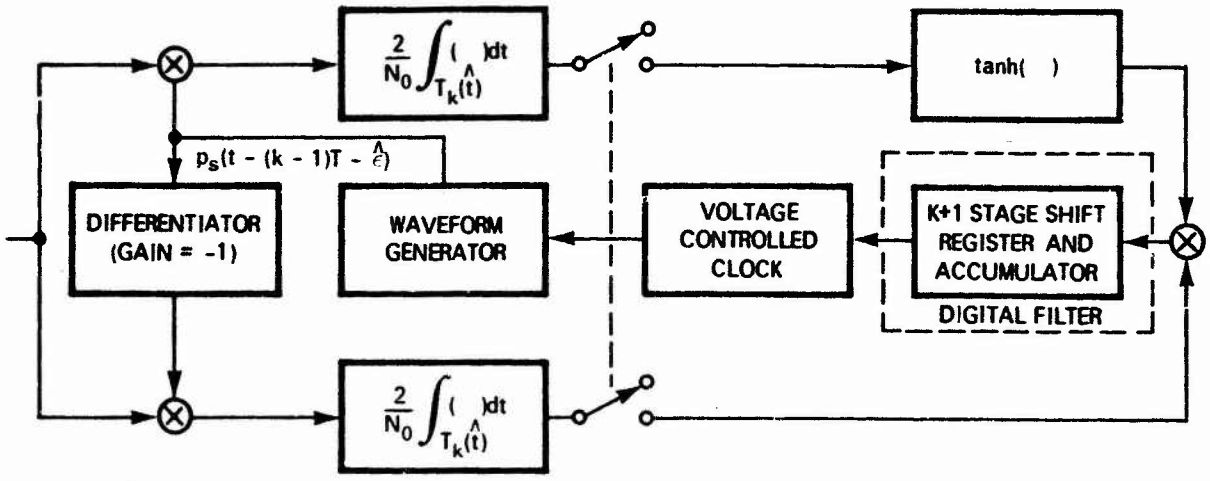

Figure VII-3. A Closed Loop Bit Synchronizer Motivated by the MAP Estimation Approach (Reference 3).

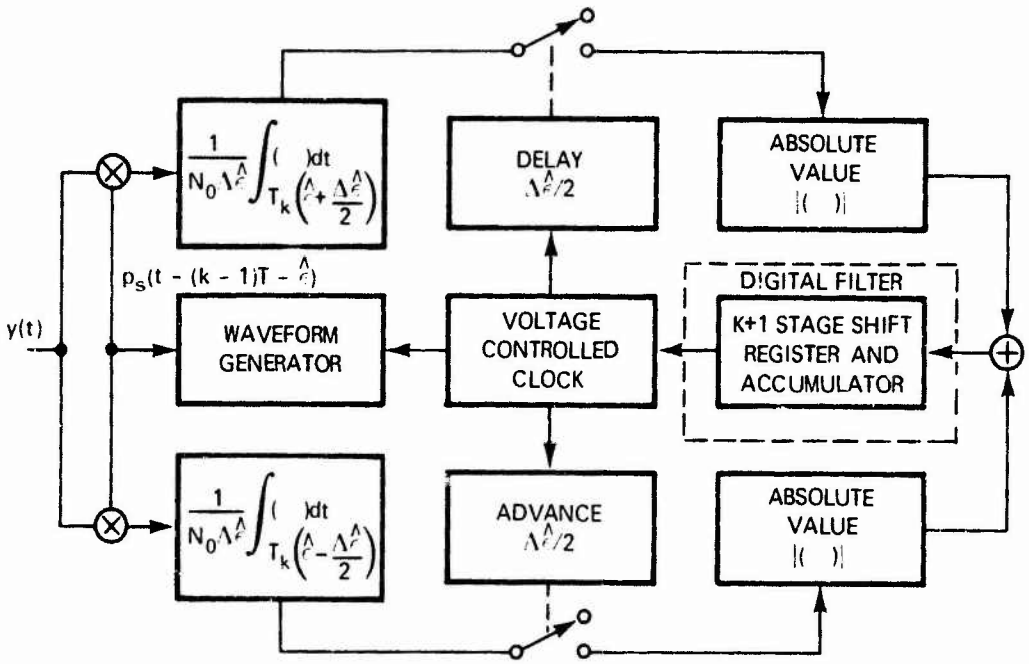

Figure VII-4. An Early-Late Gate Type of Bit Synchronizer With Absolute Value Type of Nonlinearity (Reference 3).

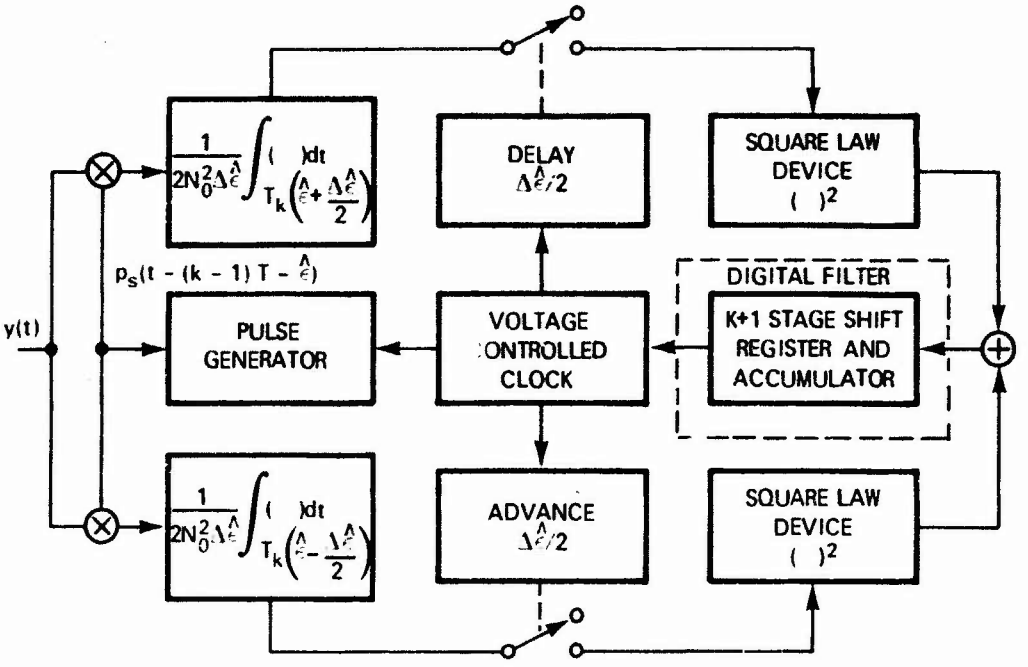

Figure VII-5. An Early-Late Gate Type of Bit Synchronizer With a Square Law Type Nonlinearity (Reference 3).

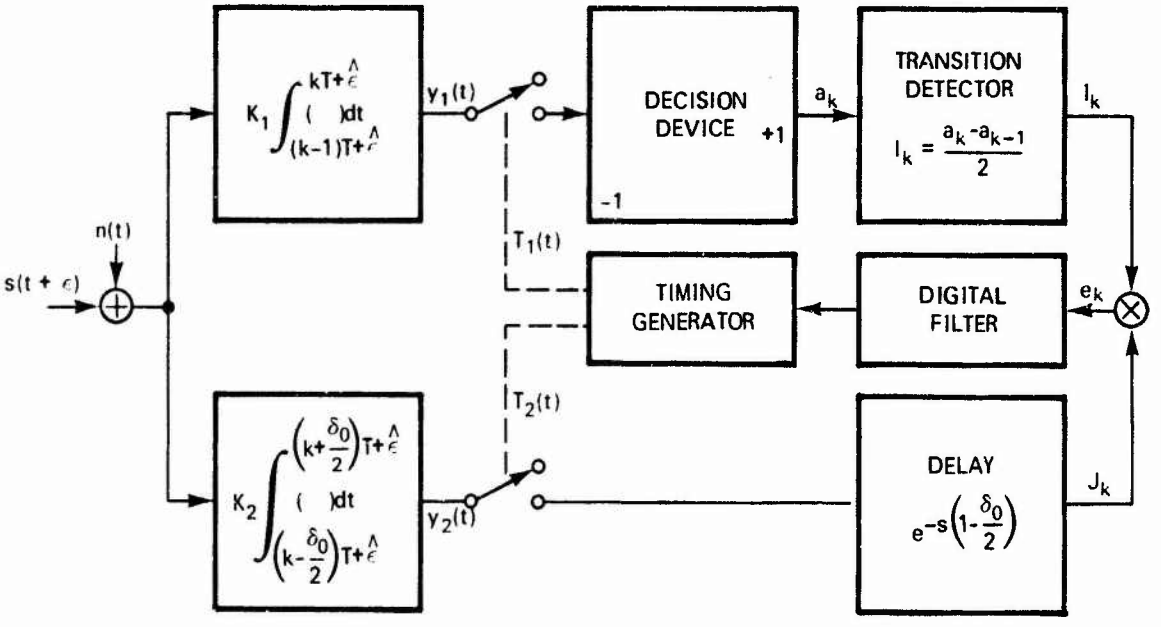

Figure VII-6. The Digital Data Transition Tracking Loop Type Bit Synchronizer (DTTL). (References 12, 13, 15, 18.)*

*Reprinted by permission of the Institute of Electrical and Electronics Engineers, Inc., 345 East 47th Street, New York, N.Y.

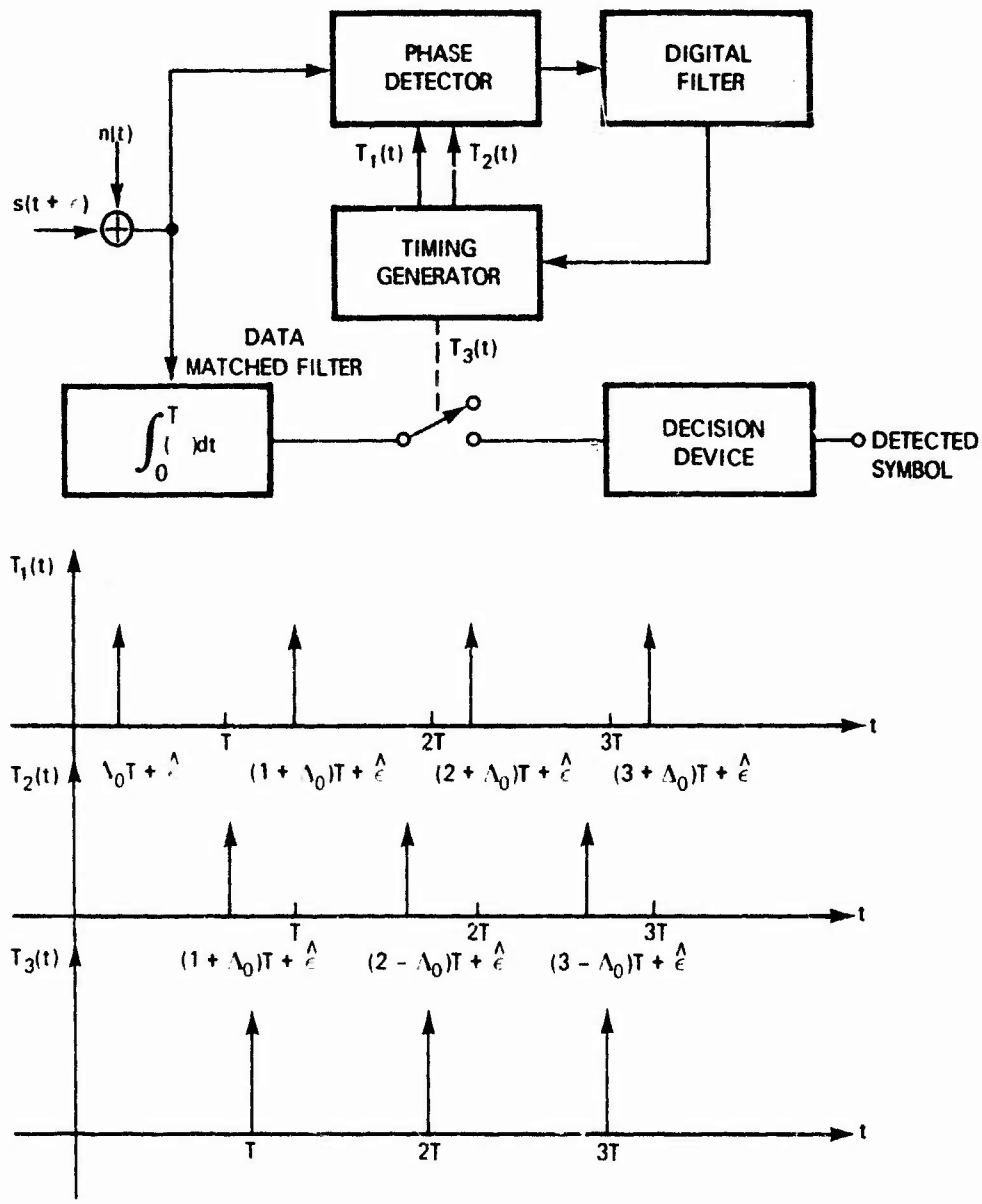

Figure VII-7. Early-Late Gate Bit Synchronizer and Associated Bit Detector. (References 3, 18.)*

*Reprinted by permission of the Institute of Electrical and Electronics Engineers, Inc., 345 East 47th Street, New York, N.Y.

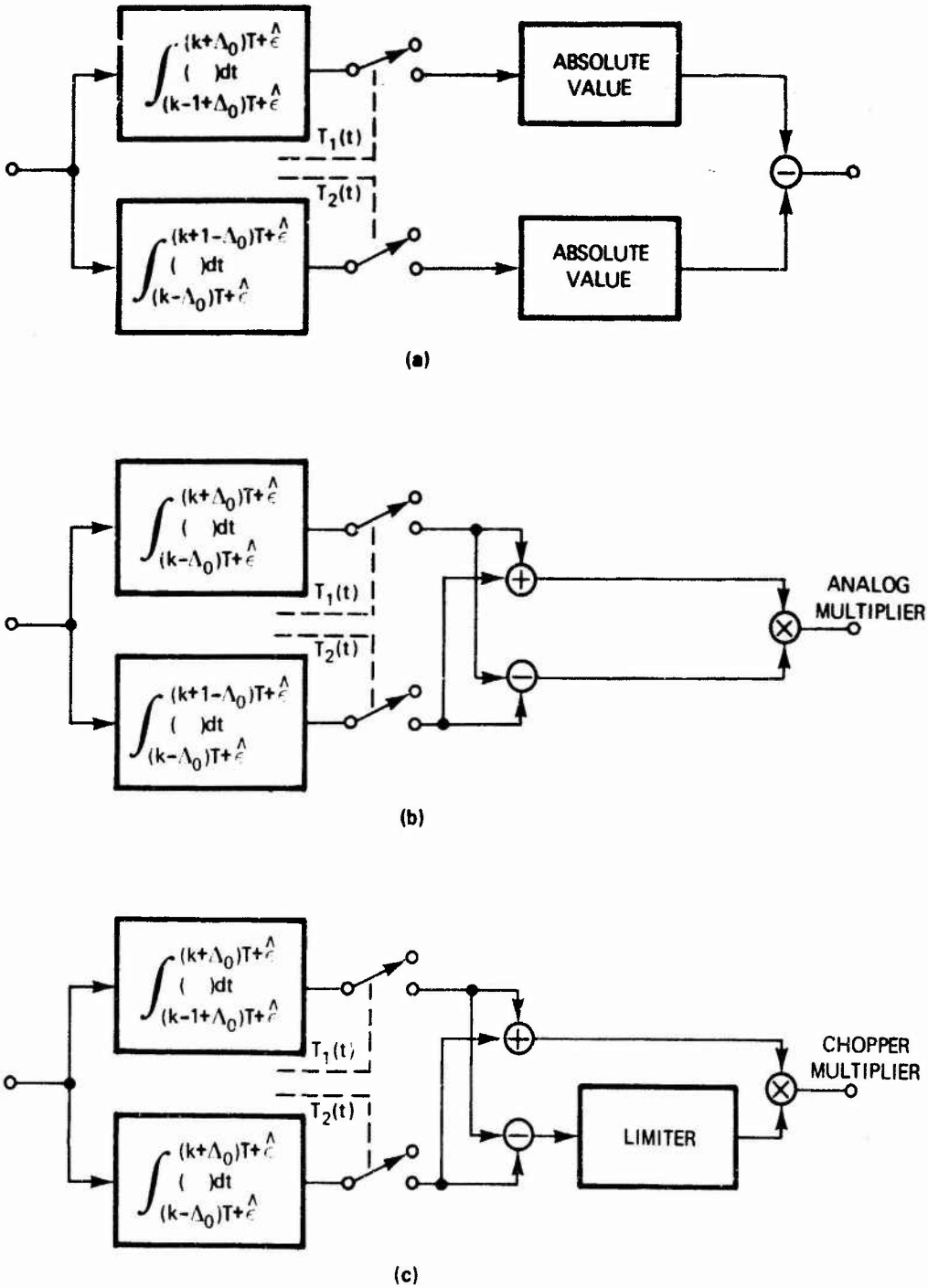

Figure VII-8. Three Different Phase Detector Topologies. (References 3, 18.)*

*Reprinted by permission of the Institute of Electrical and Electronics Engineers, Inc., 345 East 47th Street, New York, N.Y.

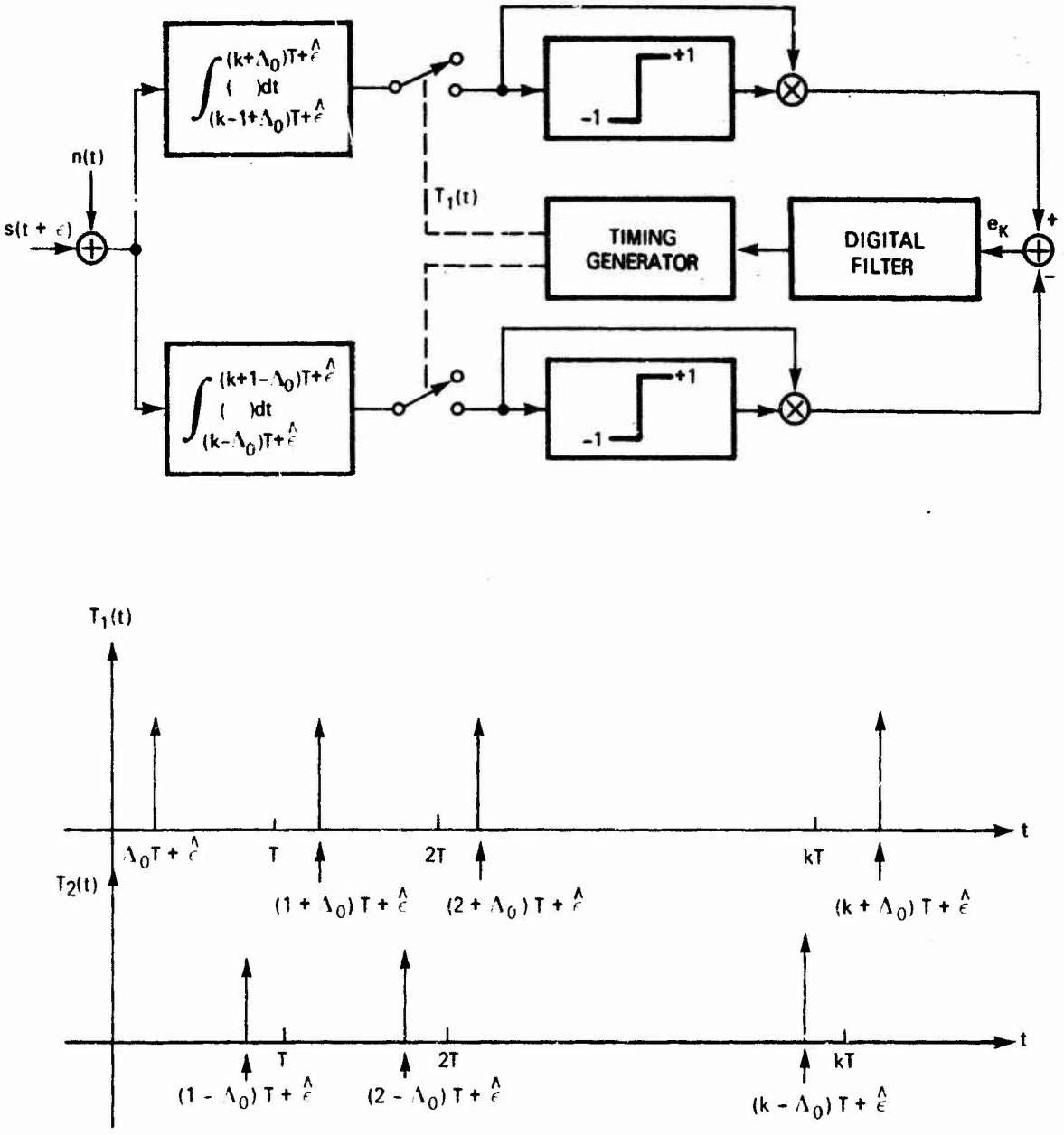

Figure VII-9. An Absolute Value Type of Bit Synchronizer (AVTS) (References 3, 18.)*

*Reprinted by permission of the Institute of Electrical and Electronics Engineers, Inc., 345 East 47th Street, New York, N.Y.

VII-1. Performance Comparison of Several BSS on the Basis of Bit Sync Jitter and Slip Time

In comparing the performance of several different BSS, one must choose a fixed operating condition that is common to all. One possible basis of comparison is on the basis of equal loop bandwidths for all configurations at every $R = ST/N_0$. This comparison is meaningful when considering the actual design of a loop having a specified bandwidth operating over a given range of input signal-to-noise ratios.

Fig. VII-10 plots the variance of the normalized bit sync jitter σ_λ^2 versus R with $\delta = 1/TW_L$ as a parameter. Included in Fig. VII-10 are the corresponding curves for the DTTL with full mid-phase integration in the error channel and the DSL. The asymptotic behaviors of σ_λ^2 for large R are described by

$$\sigma_\lambda^2 = \frac{1}{4R\delta} \; ; \; \text{AVTS}$$

$$\sigma_\lambda^2 = \frac{1}{2R\delta} \; ; \; \text{DTTL}$$

$$\sigma_\lambda^2 = \frac{5}{16R\delta} \; ; \; \text{DSL}$$

Hence, in the linear region, the absolute value type bit synchronizer offers a 3dB bit sync jitter advantage over the DTTL and a 0.97 dB advantage over the DSL type bit synchronizer. Furthermore, the AVTS appears to be uniformly better than the other two configurations at all values of the signal-to-noise ratio. If, however, one is allowed the freedom of optimizing the window width in the DTTL, then the bit sync jitter performance of the AVTS is inferior to that of the DTTL. Fig. VII-11 illustrates the performance, optimized over the window in the error channel,

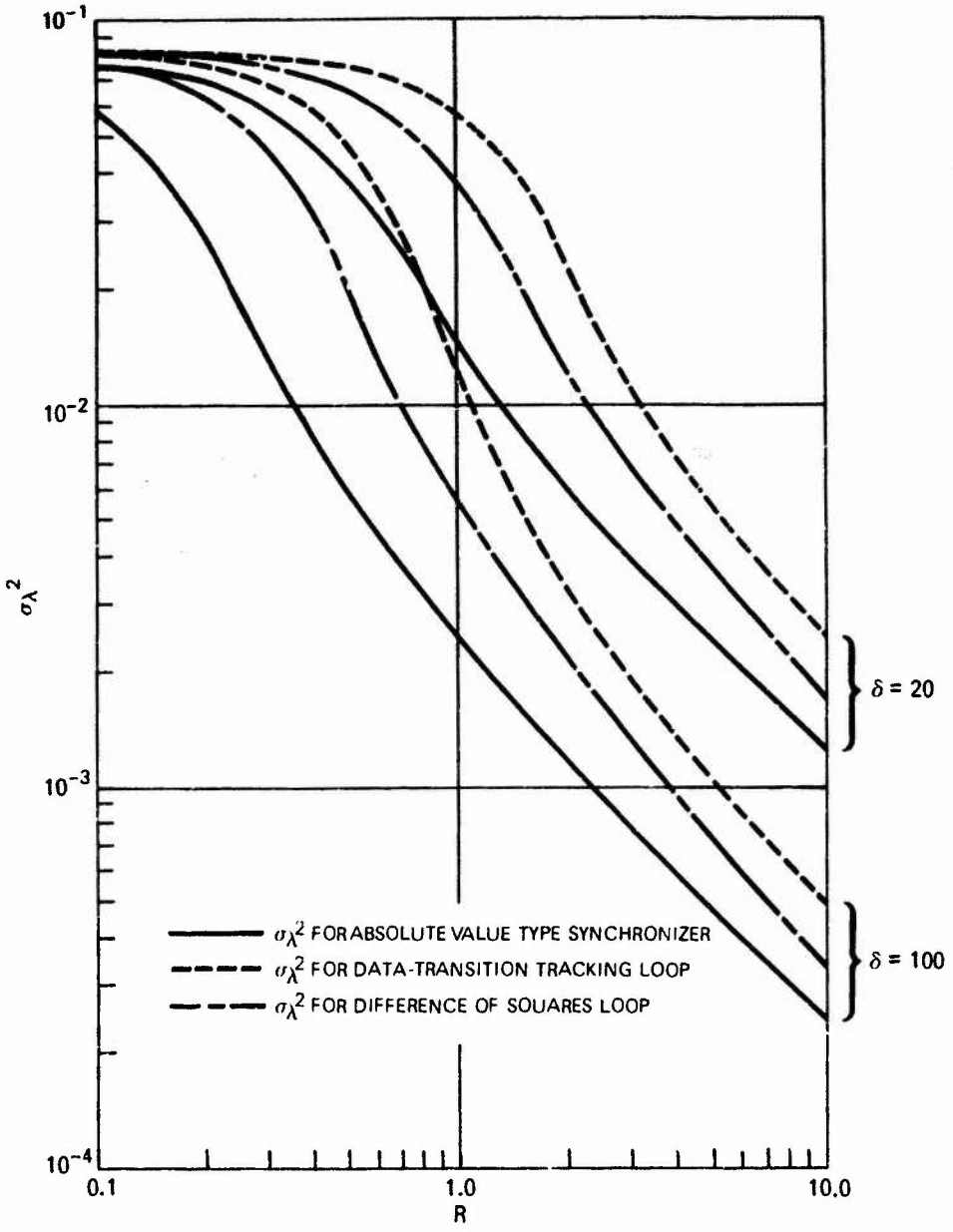

Figure VII-10. A Comparison of the Performance of Three Bit Synchronizer Configurations in Terms of Their Normalized Bit Sync Jitter. (Reference 18.)*

*Reprinted by permission of the Institute of Electrical and Electronics Engineers, Inc., 345 East 47th Street, New York, N.Y.

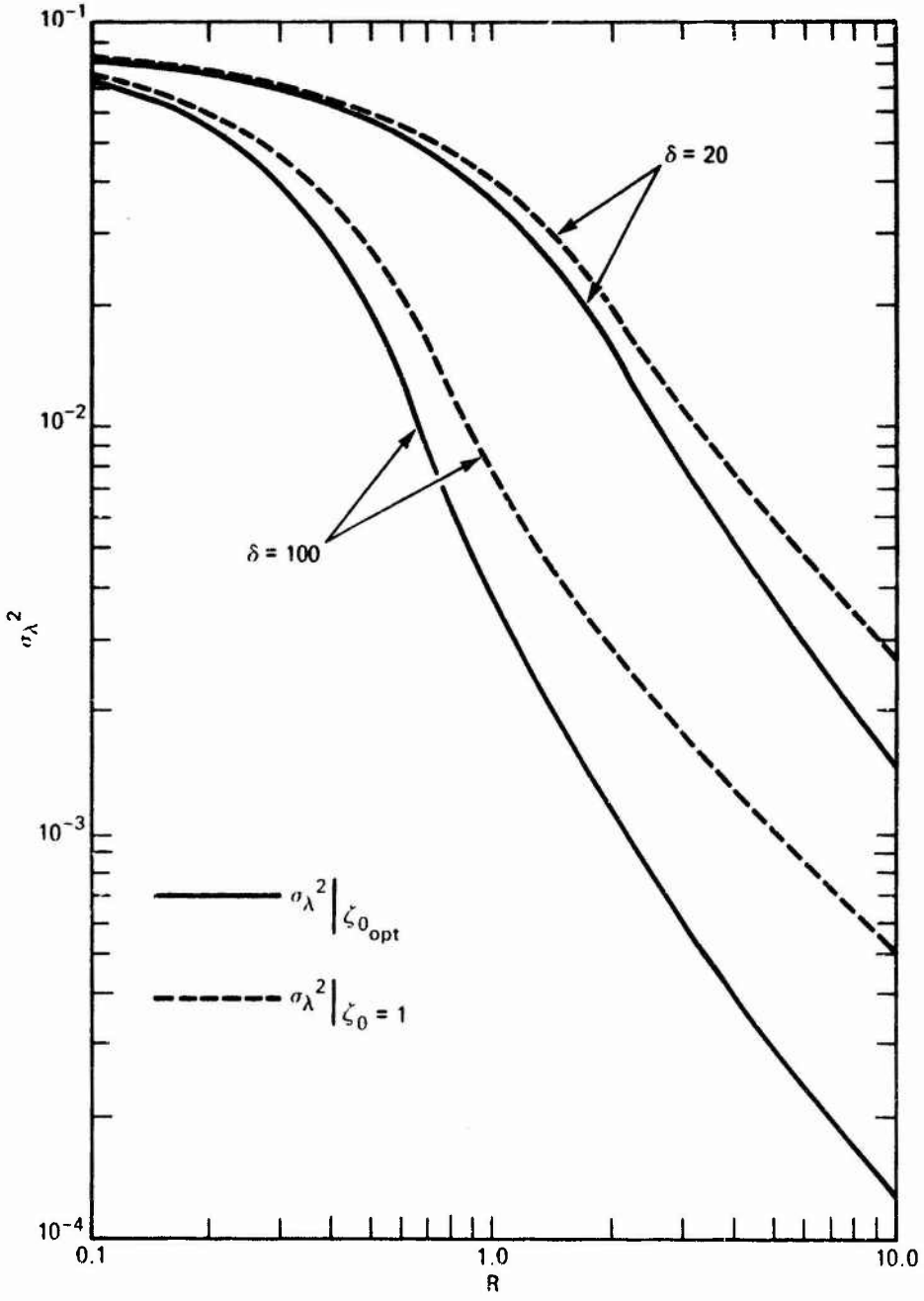

Figure VII-11. Variances of the Normalized Bit Sync Jitter Versus R for Various Values of δ; $\zeta_0 = 1$ and $\zeta_0 = \zeta_{opt}$. (Reference 18.)*

*Reprinted by permission of the Institute of Electrical and Electronics Engineers, Inc., 345 East 47th Street, New York, N.Y.

of the DTTL versus its corresponding performance when the window is full, i.e., $\xi_{10} = 1$. This figure, when compared with VII-11, confirms the above statement.

Finally, a comparison of performance on the basis of mean time to first loss of bit sync can also be made for the three BSS configuration, i.e., DTTL, AVTS, DSL. As one might suspect, the relative rankings of these three BSS remain the same as in the variance of bit sync jitter comparison just made.

VII-2. Conclusions

Several conclusions can be drawn from the results of the study thus far.

(1) The "window-optimized" DTTL is superior to the AVTS loop under the same input conditions. This is true when one considers the variance of the bit sync jitter as the measure of performance.

(2) If one considers bit slippage rate $\bar{S}$ as a measure of performance then on the basis of the phase detector characteristic which the DTTL implements versus that of the AVTS, the DTTL should have a lower bit slippage rate if the window in the error channel is optimized against the noise.

(3) No attempt has been made to evaluate the acquisition time or acquisition range of the DTTL or AVTS type BSS. This is something that would have to be accomplished by computer simulation. However, in no noise, one can conjecture from the theory given in Section VI-1 that the DTTL will perform superior to the AVTS when random NRZ data represents the input.

In summary, then, it would appear that on the basis of this study that a properly designed DTTL can outperform a AVTS in both the

tracking and acquisition mode. In fact, a digital version of the DTTL is recommended as the candidate system to construct as a computer software model. Results of computer simulation could be used to test the validity of the theory as well as serve as a basis for comparison of the performance of other BSS of interest. The digital version of the DTTL type BSS has other advantages:

(1) Data Processing in Nonreal Time

(2) Ease of Mechanization in the Digital Domain

(3) No variation in analog circuit components

(4) Loop Parameters can be switched during the acquisition and tracking mode

(5) Better stability

(6) Reliability, maintainability, and standardization

(7) Software simulations can be used to characterize and validate performance.

The major disadvantage of constructing the DTTL over the AVTS appears to be that it is more complex to implement; hence, it is more expensive to build. Finally, it should be noted that where a large quantity of BSSs are required the cost of implementing the DTTL may be reasonable.

Computer software programming for simulation of the DTTL is best begun by considering the block diagram of the system. The details of the programming can proceed on the basis of developing the behavior of the loop in terms of the random variables which appear at the output of the in-phase and quadrature integrate and dump circuits. Parameters which characterize loop performance will be acquisition time, acquisition range, bit sync jitter, BEP and bit slippage rate.

VIII. OUTPUT NOISE IN FM DISCRIMINATORS

Before attempting to characterize the output noise of an FM discriminator it is worthwhile to review the principles of operation of the discriminator type of FM receiver.

Figure VIII-1 shows the block diagram of the complete receiver. In effect, the FM discriminator receiver measures the rate of the change with respect to time, of the angle θ associated with the signal plus noise vector [(R, θ) in polar coordinates, (c, s) in rectangular coordinates] as shown in Fig. VIII-2. The equations for the basic voltages in the FM discriminator are given below (see Fig. VIII-1):

1. Input to the receiver

$$v = A \cos \left(\omega_c t + \int m \right) + n(t) \tag{1}$$

$$\int m \triangleq \int^t m(\tau) d\tau \tag{2}$$

$$n(t) \triangleq Ax(t) \cos \omega_c t - Ay(t) \sin \omega_c t \tag{3}$$

x and y are normal $(0, \sigma)$ Gaussian r.v.'s.

2. Input to Limiter

$$e_1 = Ac \cos \omega_c t - As \sin \omega_c t \tag{4}$$

$$s \triangleq \sin \int m + y/A \tag{5}$$

$$c \triangleq \cos \int m + x/A \tag{6}$$

x, y are noise with bandwidth ω_n.

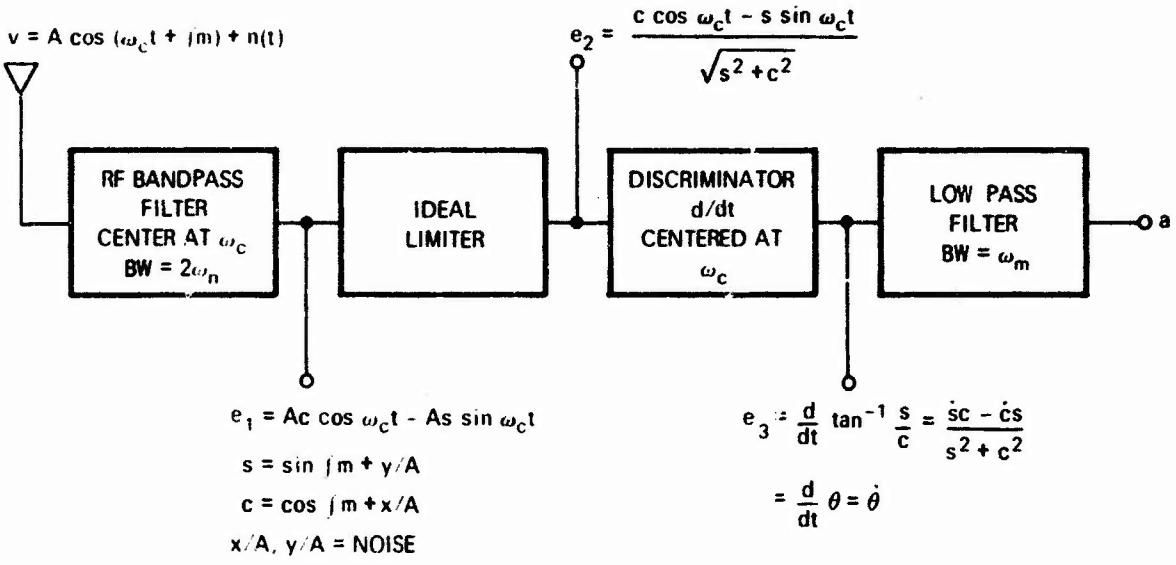

Figure VIII-1. Block Diagram of the FM Discriminator.

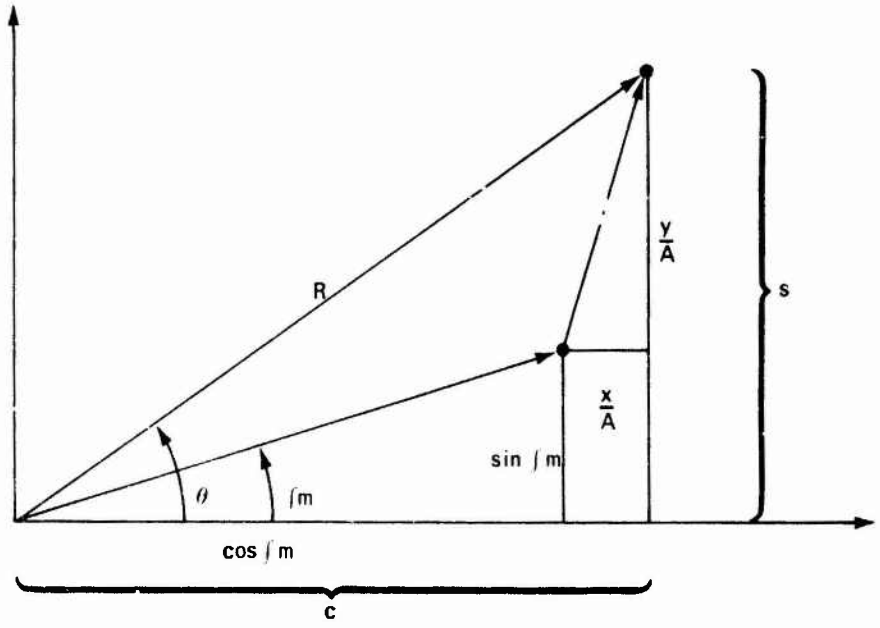

Figure VIII-2. Signal and Noise Vectors in the FM Discriminator.

3. **Input to the discriminator**

$$e_2 = \frac{c \cos \omega_c t - s \sin \omega_c t}{\sqrt{s^2 + c^2}} \tag{7}$$

4. **Input to the low pass filter**

$$e_3 = \frac{d}{dt} (\tan^{-1} \frac{s}{c}) = \frac{\dot{s}c - \dot{c}s}{s^2 + c^2} \tag{8}$$

For example, for sine wave modulation, the receiver is

$$v(t) = S(t) + n(t) = A \cos(\omega_c t + \beta \sin \omega_m t) + Ax \cos \omega_c t - Ay \sin \omega_c t$$

$$S(t) + n(t) = R(t) \cos \left(\omega_c t + \beta \sin \omega_m t + \tan^{-1} \left(\frac{y \cos \varphi - x \sin \varphi}{1 + x \cos \varphi + y \sin \varphi} \right) \right)$$

where $\varphi = \beta \sin \omega_m t$ and

$$R(t) = \sqrt{(1 + x \cos \varphi + y \sin \varphi)^2 + (y \cos \varphi - x \sin \varphi)^2}$$

The output is given by

$$\frac{d}{dt} \left[\beta \sin \omega_m t + \tan^{-1} \left(\frac{y \cos \varphi - x \sin \varphi}{1 + x \cos \varphi + y \sin \varphi} \right) \right]$$

$$\approx \beta \omega_m \cos \omega_m t + \underbrace{\frac{d}{dt} [y \cos \varphi - x \sin \varphi]}_{n_g = \text{gaussian noise}} + \text{spikes} + \text{doublets}$$

with the first two terms being the signal and the Gaussian noise respectively. In what follows we shall investigate the statistical characteristics of the spike component present in the output as well as discuss the qualitative apsects of the outputs.

Fig. VIII-3 shows typical input and output waveforms for an FM discriminator at high and low β with the noise bandwidth (ω_n) and the carrier-to-noise ratio (CNR) fixed. In addition, the modulation shown is assumed to be sinusoidal, i.e., $m = \beta\omega_m \cos \omega_m t = \omega_n \cos \omega_m t$ since $\beta \triangleq \omega_n/\omega_m$. Studies of these waveforms (which are readily observed on an oscilloscope) have led various investigators such as Rice (Ref. 19), Cohn (Ref. 20) and Hill (Ref. 21) to describe the output of the FM discriminator as consisting of the following components:

1. Modulation
2. Gaussian Noise
3. Doublets (with area zero) or Additive Noise
4. Spikes (with area 2π) or Subtractive Noise (sometimes called clicks)

The first component is the transmitted information. The last three components are the three types of noise which can occur with various signal vector-noise vector configurations. Fig. VIII-4 shows the type of situation which produces Gaussian noise in θ and $\dot{\theta}$, i.e., when the amplitude of the noise vector is much less than the amplitude of the signal vector (fixed at unity amplitude). For simplicity, the modulation has been set to zero. When the noise vector is large and comes close to the origin (0), but does not circle the origin as in Fig. VIII-5, the discriminator output contains a doublet. Note that the net change in θ, $\theta_2 - \theta_1$, is $\ll 2\pi$. When the noise vector is large and does circle the origin, we have a spike. This condition is shown in Fig. VIII-6. Note that in this case the net change in θ is approximately 2π.

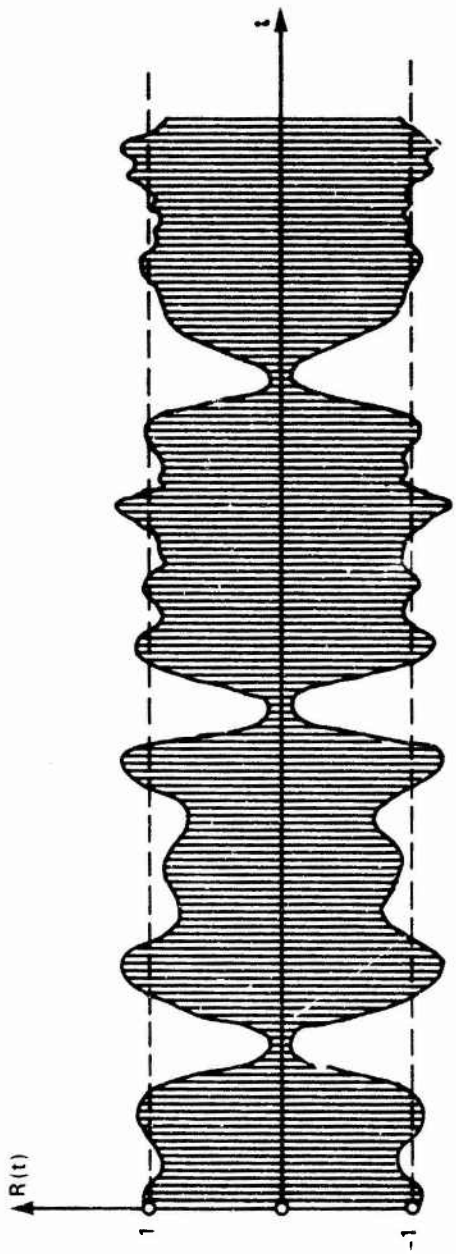

Figure VIII-32. Typical Graph of the Signal Plus Noise Vector Versus Time.

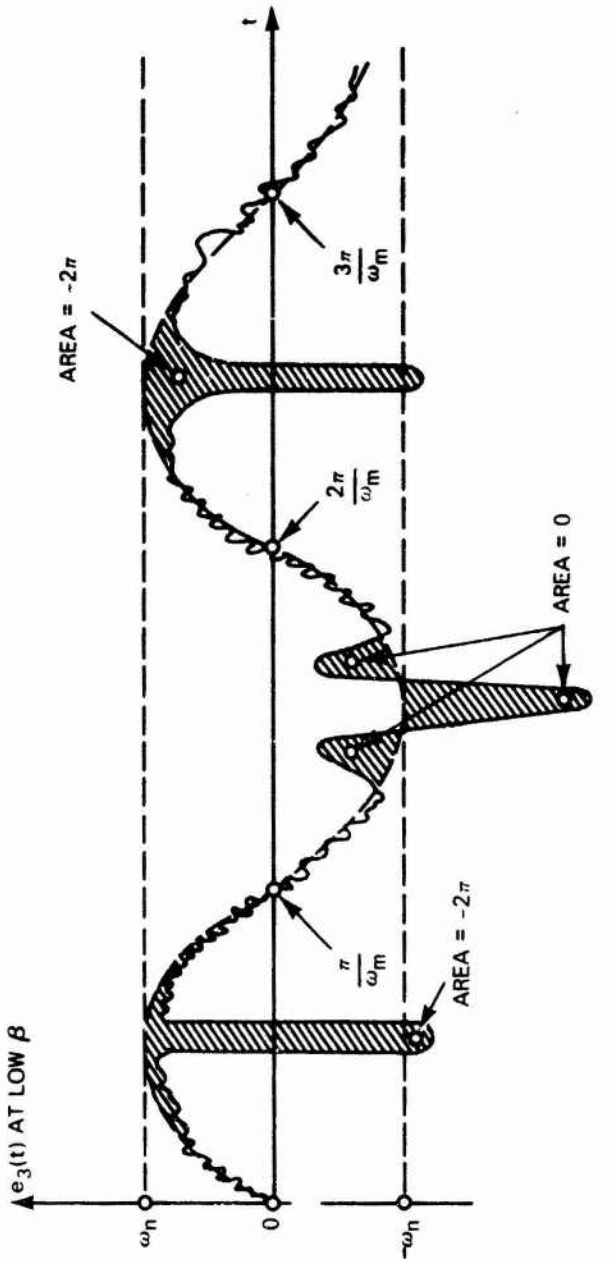

Figure VIII-3b. Typical Graph of the Discriminator Output Versus Time at Low β.

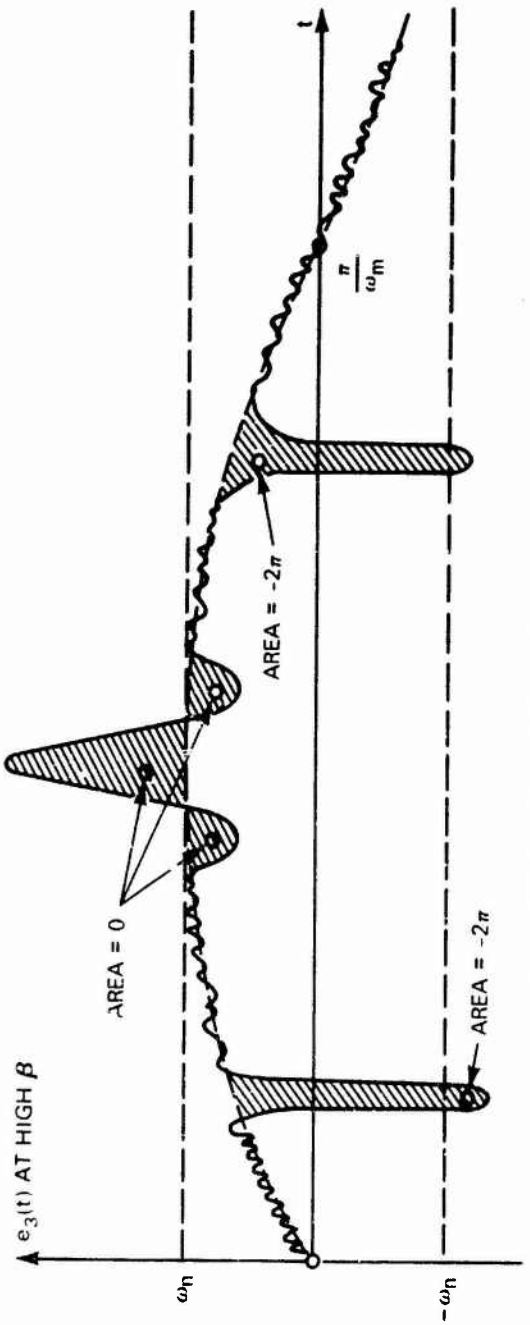

Figure VIII-3c. Typical Graph of the Discriminator Output.

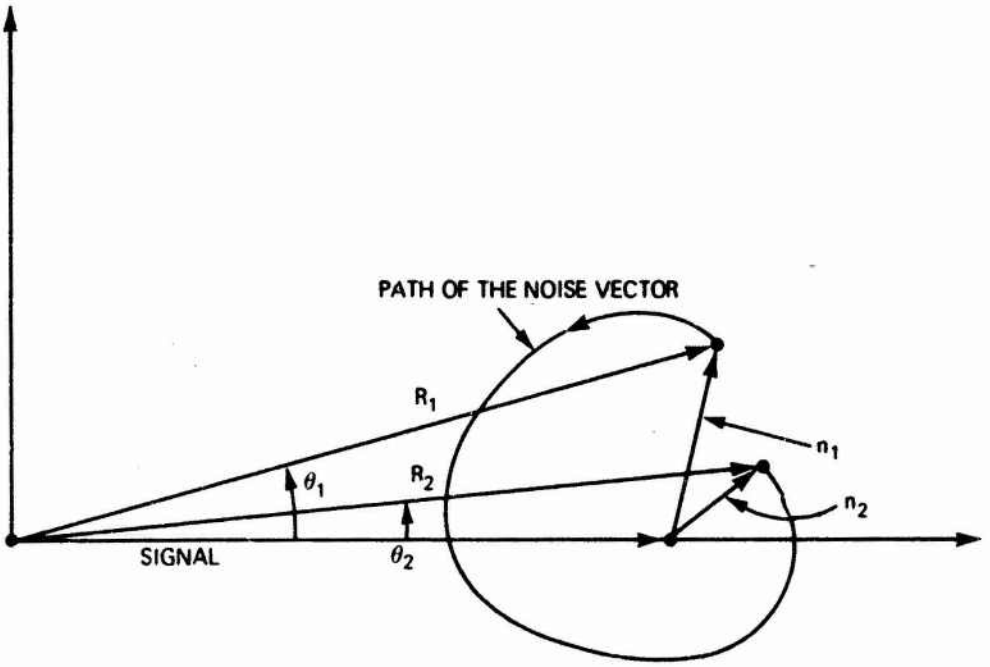

Figure VIII-4. Noise Vector Path for Gaussian Noise.

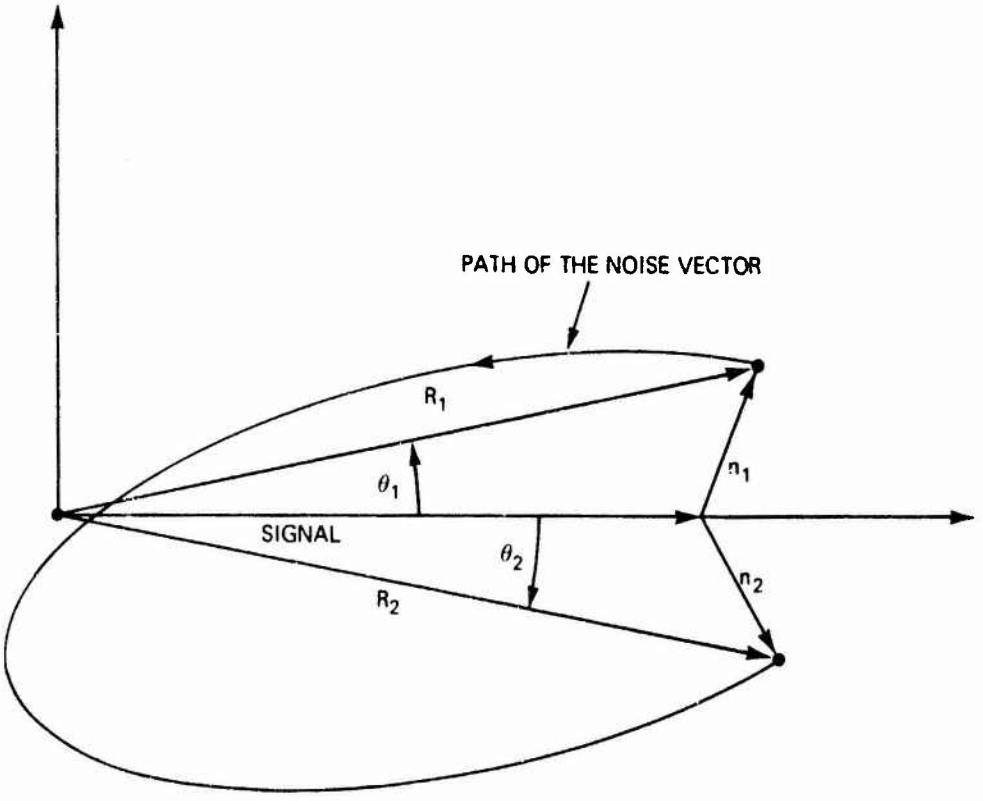

Figure VIII-5. Noise Vector Path for a Doublet.

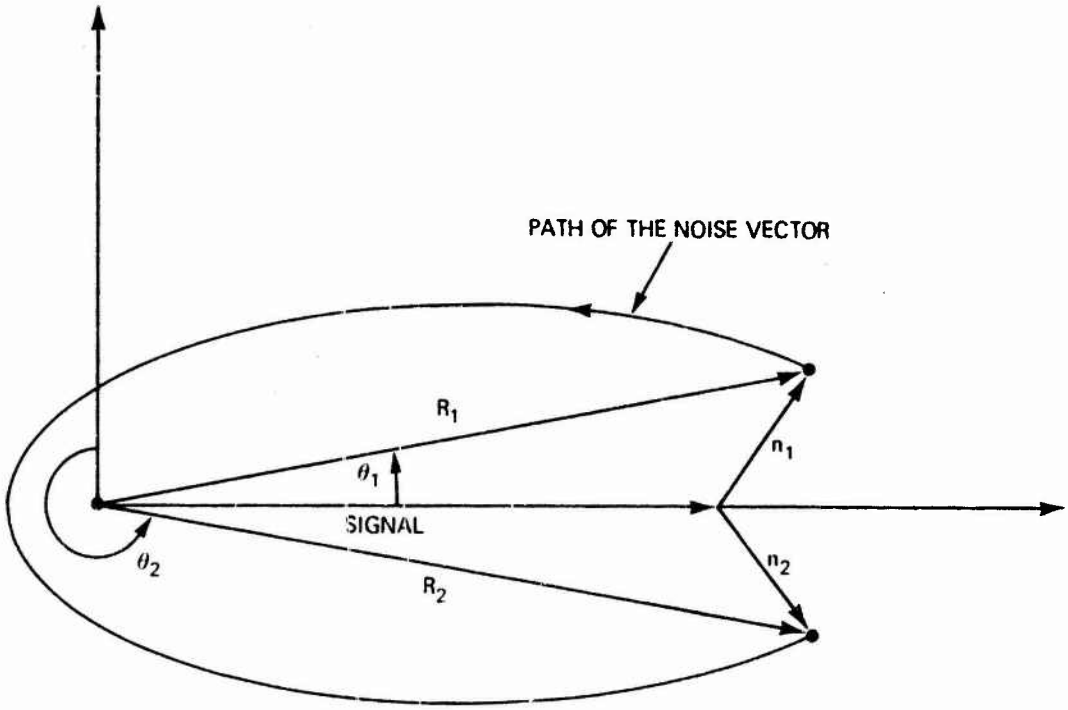

Figure VIII-6. Noise Vector Path for a Spike.

The approximate spectrums of each of the four components at the output of the discriminator are shown in Figs. VIII-7a, b, c and d. The spectrum of of the modulation is chosen as rectangular for simplicity. The spectrum of the Gaussian noise is obtained by noting that the Gaussian noise is approximately

$$n_g = \frac{d}{dt}\left(y \cos \int m - x \sin \int m\right) \tag{9}$$

at the output of the discriminator. Evaluating the autocorrelation function of $y \cos \int m - x \sin \int m$, we find that

$$E\left[\left(y_1 \cos \int m_1 - x_1 \sin \int m_1\right)\left(y_2 \cos \int m_2 - x_2 \sin \int m_2\right)\right] \tag{10a}$$

$$= 2R_x(\tau)R_{\cos \int m}(\tau) \tag{10b}$$

$$= R_g(\tau) \tag{10c}$$

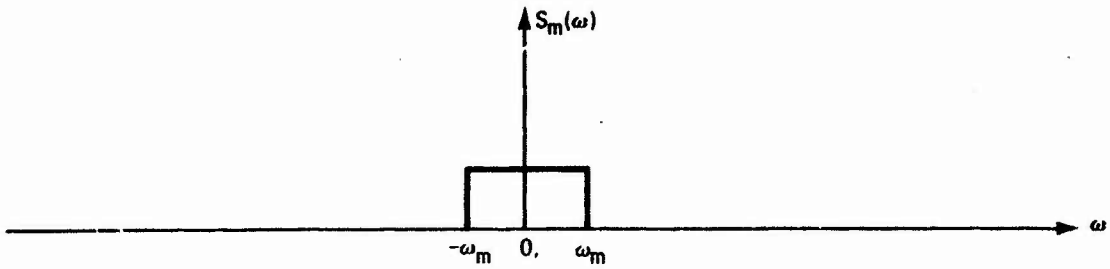

Figure VIII-7a. Spectrum of the Modulation.

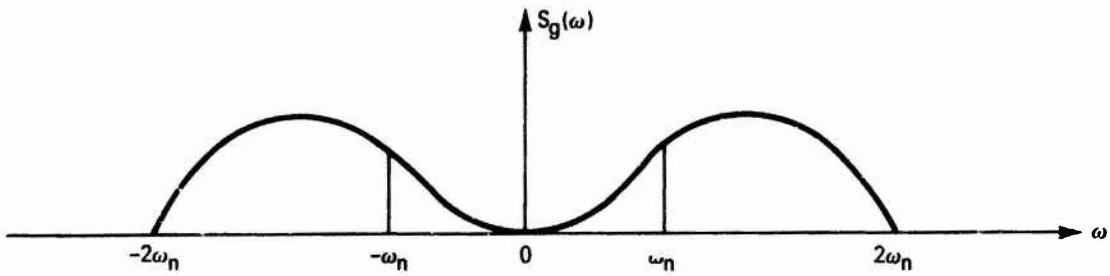

Figure VIII-7b. Spectrum of the Gaussian Noise.

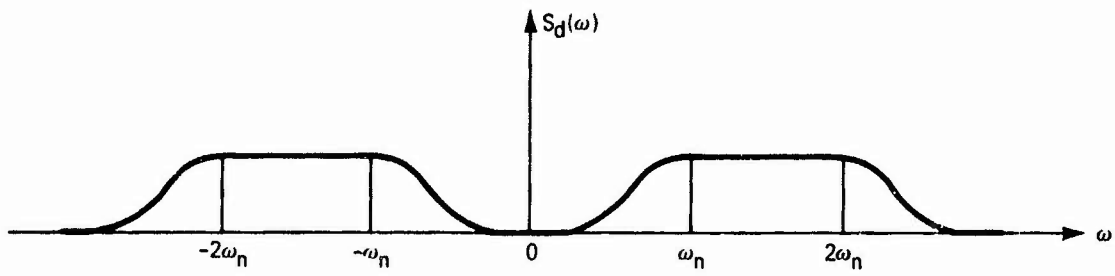

Figure VIII-7c. Spectrum of the Doublet Noise.

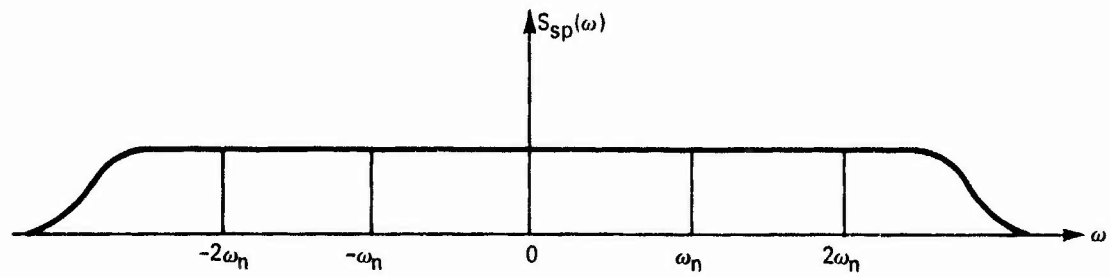

Figure VIII-7d. Spectrum of the Spike Noise.

since

$$E(x_1 x_2) = E(y_1 y_2) = R_x(\tau) \tag{11}$$

$$E(x_1 y_2) = E(x_2 y_1) = 0 \tag{12}$$

$$E\left(\cos \int m_1 \cos \int m_2\right) = E\left(\sin \int m_1 \sin \int m_2\right) = R_{\cos \int m}(\tau) \tag{13}$$

For simplicity, one can assume that

$$S_x(\omega) = \begin{cases} \dfrac{N_0}{2A^2} & |\omega| < \omega_n \\ 0 & |\omega| > \omega_n \end{cases} \tag{14}$$

and that

$$S_{\cos \int m}(\omega) = \begin{cases} \dfrac{\pi}{2\omega_n} & |\omega| < \omega_n \\ 0 & |\omega| > \omega_n \end{cases} \tag{15}$$

The latter assumption is based on the fact that

$$E\left(\cos \int m\right)^2 = 1/2 \tag{16}$$

and that the bandwidth of the modulated carrier is the same as the bandwidth of the noise. Thus,

$$S_g(\omega) = 2\omega^2 S_x(\omega) * S_{\cos \int m}(\omega) \tag{17}$$

where the ω^2 factor is introduced by the d/dt operator in (9). Evaluating the convolution in (17), one finds that

$$S_g(\omega) = \begin{cases} \frac{N_0}{2A^2}\,\omega^2\left[1 - \frac{|\omega|}{2\omega_n}\right], & |\omega| < 2\omega_n \\ 0 & |\omega| > 2\omega_n \end{cases} \tag{18}$$

The spectra of the spike noise and the doublet noise are not known exactly. The best one can do is approximate them by assuming that the spikes and doublets have typical shapes like those shown in Fig. VIII-8. [However, wide variations from these shapes occur.] The doublet waveform indicates that the spectrum is bandlimited and has a parabolic shape at the origin. Thus its presence can be largely removed by the output filter. The spike waveform indicates that the spectrum is also bandlimited but is flat at the origin. It is assumed in both cases that the sequences of

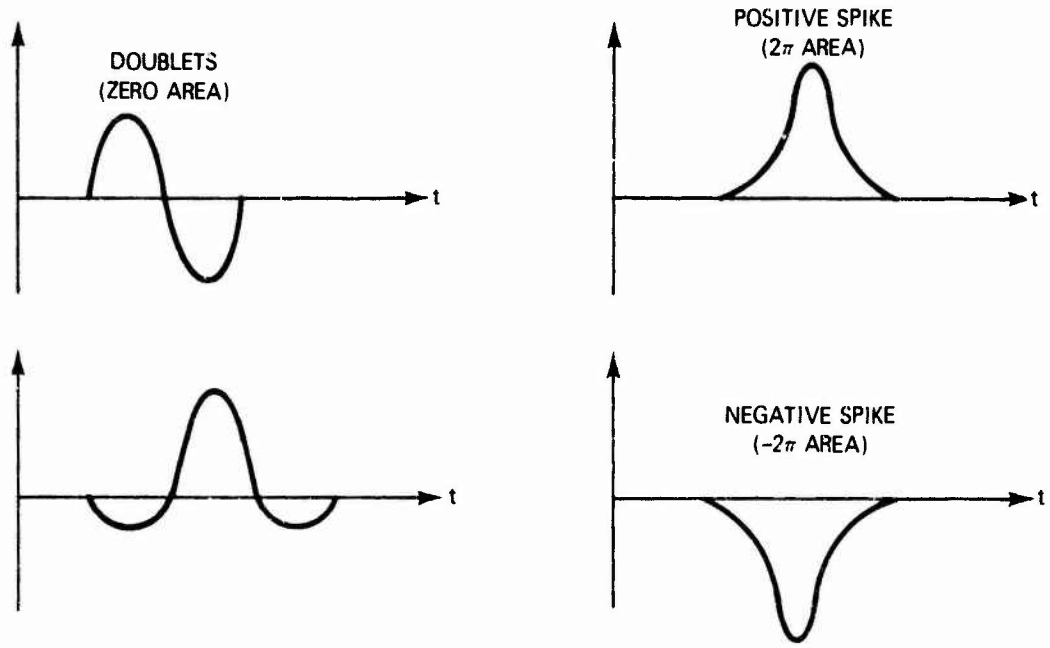

Figure VIII-8. Typical Shapes of Spikes and Doublets.

doublets and spikes at the output of the discriminator occur randomly and have a finite probability of occurrence. Hence, their occurrence is characterized by a probability density function.

If we let N(T) be a random variable which denotes the number of spikes that occur in time T. Assuming, (in accordance with Rice) that the spikes are independent and that those tending to increase (decrease) θ by 2π form a Poisson process with rate of occurrence $N_+(N_-)$. In general, when modulation is present, N_+ and N_- are not equal. The probability density of $z = N(T)$ is given by

$$p(z) = \exp\left[-(N_+ + N_-)T\right] \sum_{k=-\infty}^{\infty} \delta(z-k)\left(\frac{N_+}{N_-}\right)^{k/2} I_k(2T\sqrt{N_+ N_-}) \qquad (19)$$

as can be shown by forming the discrete convolution of the densities of the positive and negative spikes. In (19) $\delta(x)$ is the Dirac delta function and $I_k(\mu)$ is the modified Bessel function of integer order k.

If one is concerned with the type of modulation in which the instantaneous frequency deviates from the carrier frequency by ω_m rad/sec for a time T then Rice shows that the average rates N_+ and N_- when the noise at the receiver input is Gaussian (Ref. 19)

$$N_+ = \tfrac{1}{2}\{\sqrt{r^2 + f_m^2}\left[1 - \operatorname{erf}(\sqrt{\rho + \rho f_m^2/r^2}\right] - f_m \exp(-\rho)\left[1 - \operatorname{erf}(f_m\sqrt{\rho/r})\right]\} \qquad (20)$$

and

$$N_- = N_+ + f_d \exp(-\rho) \qquad (21)$$

where

$$\rho = A^2/2\sigma_n^2 = \text{SNR at IF output}$$

$$r = \frac{1}{2\pi}\left[\frac{\dot{\sigma}}{\sigma}\right] \approx \frac{f_n}{\sqrt{2}}$$

$$\sigma^2 = \text{var } x(t) = \text{var } y(t) \qquad (22)$$

$$\dot{\sigma}^2 = \text{var } \dot{x}(t) = \text{var } \dot{y}(t)$$

Under the assumption that f_m is positive we have asymptotically

$$N_+ \sim \frac{1}{4\sqrt{\pi}} \frac{1}{\rho^{3/2}} \frac{r}{\left(1 + \frac{f_m^2}{r^2}\right)\left(\frac{f_r^2}{r^2}\right)} \exp\left[-\rho\left(1 + f_m^2/r^2\right)\right] \qquad (23)$$

$$N_- \sim N_+ + f_m \exp(-\rho)$$

Thus, we see that for large ρ an ever majority of spikes occur in the "negative direction" ($f_m > 0$) giving rise to the substractive noise. In fact, for large ρ

$$\left.\begin{aligned} N_+ &\sim 0 \\ N_- &\sim f_m \exp(-\rho) \end{aligned}\right\} f_m > 0 \qquad (24)$$

For $f_m < 0$ the situation is reversed of course. Thus we observe that the effect of the spikes on a modulated carrier is to tend to make the measured frequencies appear "closer" to the carrier frequency than the transmitted frequencies. That is, confining oneself, for the moment, to only error caused by spikes, frequencies transmitted higher (lower) than the carrier will be measured (by the discriminator) to be at that frequency or a lower (higher) one when the noise is small.

If one is willing to make the approximation given in (24) then the probability density function for z = N(T) can be approximated by the Poisson distribution

$$p[N(T)] \sim \frac{\exp[-N_- T](N_- T)^{N(T)}}{[N(T)]!} \qquad (f_m > 0)$$

$$N(T) = 0, 1, 2, \ldots \tag{25}$$

when $(f_m > 0)$.

Next we characterize the spectral properties of the output spike noise. This can be accomplished as follows: Let the spikes be modeled as random pulses of width ϵ, height $\pm 2\pi/\epsilon$ and rate N_s (spikes/second) = $N_+ + N_-$, as in Fig. VIII-9. The autocorrelation function for the spike process is illustrated in Fig. VIII-10. The power spectral density of the spike process is given by

$$S(\omega) = \frac{4\pi^2 N_s}{\epsilon^2} \cdot \frac{4 \sin^2(\omega\epsilon/2)}{\omega^2}$$

$$S(\omega) = 4\pi^2 N_s \left[\frac{2 \sin(\omega\epsilon/2)}{\omega\epsilon}\right]^2 \tag{26}$$

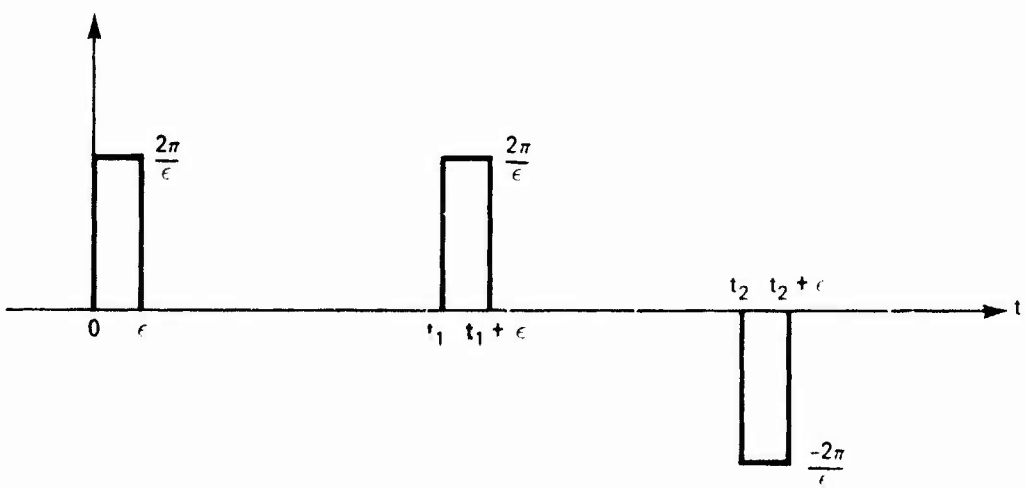

Figure VIII-9. Approximation of Spikes With a Series of Random Pulses.

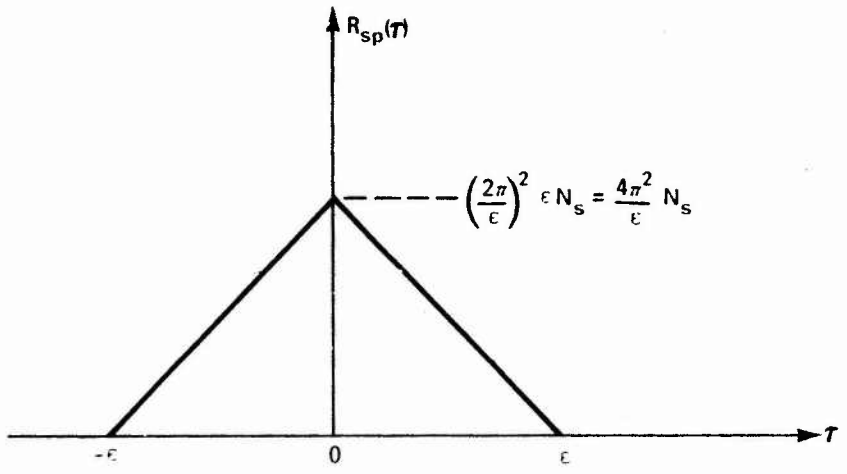

Figure VIII-10. Autocorrelation Function of a Series of Random Pulses.

If ϵ is small then the output filter sees a power spectrum, due to the spike noise, on the order of

$$S(\omega) \approx 16\pi^2 N_s \tag{27}$$

so that the output power due to the spike noise is

$$N_{spike} = 16\pi^2 (N_+ + N_-) f_m \tag{28}$$

where ω_m is the output bandwidth. What this says is that the energy in the spike noise is spread over a wide frequency range and this range is wider than the modulation bandwidth and wider than the input noise bandwidth. In fact, the equivalent effect of spikes on the performance of any bit synchronization system is to drastically raise the value of the noise spectral density at the origin. It would be interesting to characterize the probability density function of the bit sync error when the system input consists of Gaussian noise plus spikes.

Performance Comparisons of FM Discriminators and Matched Filters

If one assumes perfect bit sync the BEP using the FM discriminator and a matched filter type detector are compared in Fig. VIII-11 when on is transmitting an alternating sequence of frequencies. Notice that in the region of small β, i.e., $\beta \leq 0.734$) the matched filter and the FM discriminator display comparable BEP. This is in the region where the additive Gaussian noise effects the BEP. When the BEP using the FM discriminator results principally from spikes $0.734 < \beta < 4.24$, the matched filter is seen

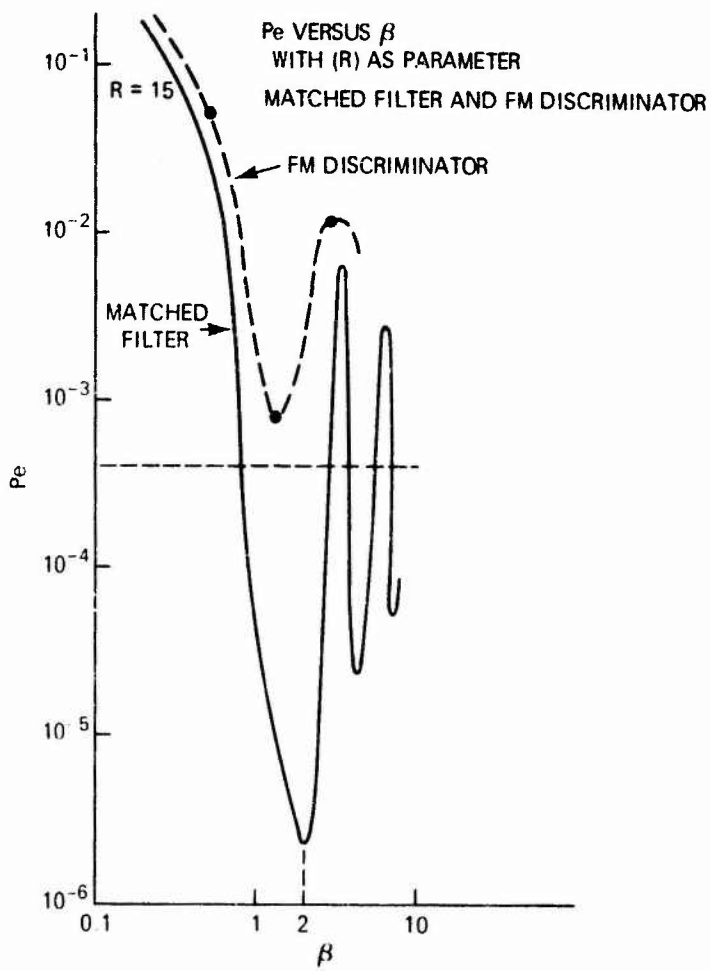

Figure VIII-11. Comparison of the Matched Filter and FM Discriminator. (Reference 22.)*

*Reprinted by permission of the Institute of Electrical and Electronics Engineers, Inc., 345 East 47th Street, New York, N.Y.

to have a substantially lower BEP. It is also observed that the minimum BEP occurs when $\beta \approx 2$ for the matched filter detector while the minimum for the FM discriminator occurs when $\beta \approx 1$. Other theoretical and experimental comparisons of BEP vs modulation index are illustrated in Fig. VIII-12 when bit sync is perfect. Lowering of the FM threshold can be accomplished through

1. Employing FM with Feedback
   a. Discriminator (FMFB)
   b. PLL
2. Matched filter Detect rather than Lowpass Filter and Sample
3. Spike Detection and Compensation.

Spike noise detection and elimination offers an advantage in flexibility since it is not a demodulator, but, rather a device which can be implemented at the output of any FM discriminator. The improvement in threshold performance seems to be on the order of 1.5 to 2 dB while the PLL type discriminator offers approximately a 3 dB threshold advantage over the frequency discriminator. The combined effects of spike detection and elimination with PLL discriminator would then lower the threshold by 4 to 5 dB. Spike detection and elimination circuits combined with FMFB probably offers a 3 to 4 dB reduction in the threshold effect.

Computer Simulation

Since the output noise in an FM discriminator is impossible to characterize in any exact sense, and since the effects due to the noise are unique to the system with which the bit synchronizer electronics is to operate; they should be simulated as closely as is practical in order to

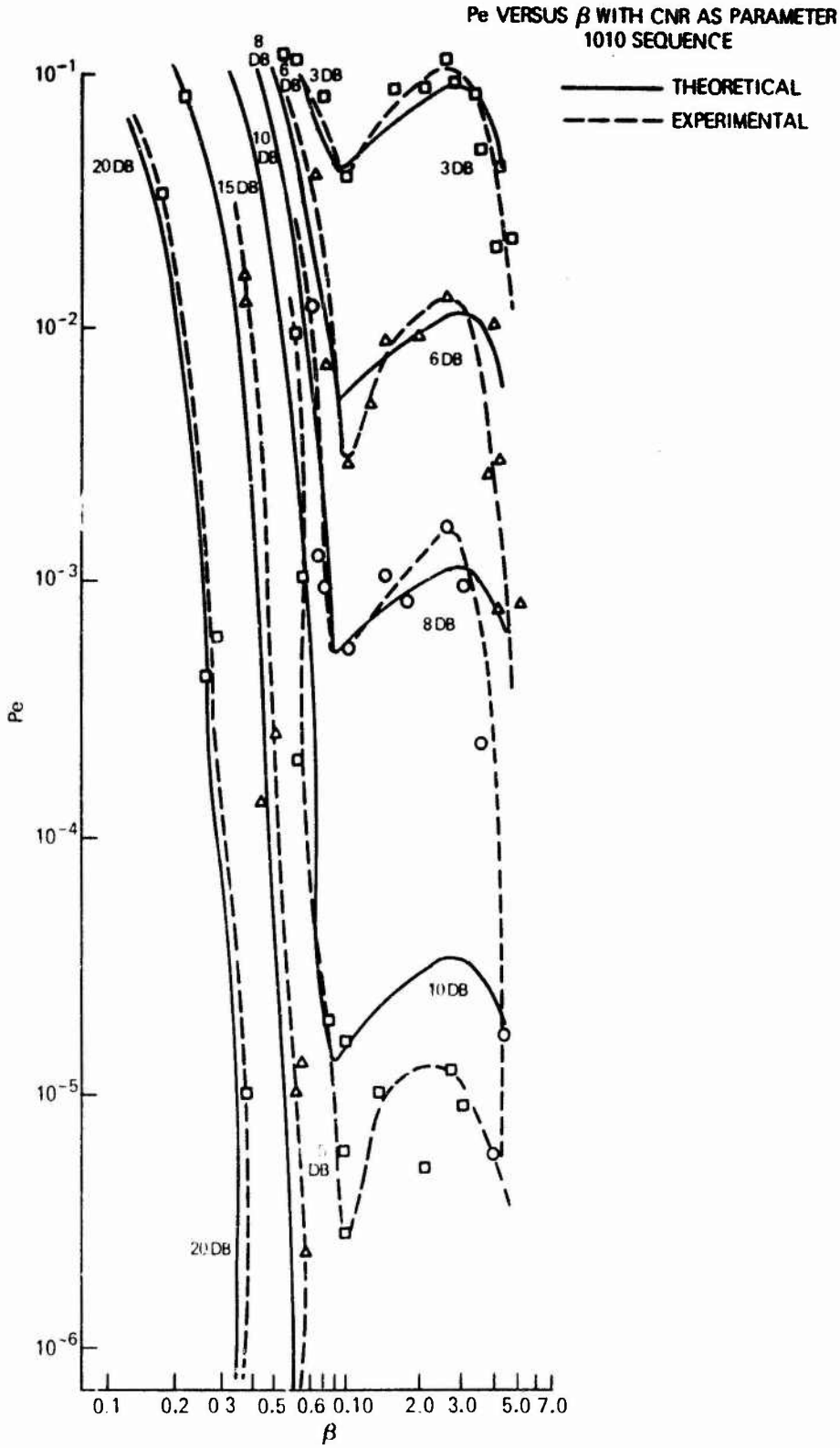

Figure VIII-12. Theoretical and Experimental Comparison of Error Probability as a Function of Modulation Index. (Reference 22.)*

*Reprinted by permission of the Institute of Electrical and Electronics Engineers, Inc., 345 East 47th Street, New York, N.Y.

determine the performance of the bit synchronizer as well as bit detector in the presence of such phenomena. A simulation in which the signal is summed with the outputs of a Gaussian and spike (Poisson) noise generator which are calibrated by the above equations may perhaps be too coarse a representation to determine overall performance; therefore, one may be forced to simulate all subsystems in the overall receiver and determine their combined performance.

Time domain computer simulation techniques are directly applicable to problems wherein system analysis is formidable. The analog computer can be used for certain problems as can the digital computer. However, each method has its particular problems, commonly including run time and complexity of problem set-up. Simulation of communication links employing FM can be readily accomplished. Computation can be done at baseband frequencies so that the sample frequencies are not determined by the carrier frequency. Nonsymmetric bandpass filters can be accurately represented by using bilinear z-transform methods while the results given in Ref. 20 can be used to model and simulate the discriminator. If such an approach is used one avoids having to model the discriminator output noise directly so that the thermal noise in the channel is all that is required to model. There exists Gaussian random number generators which readily accomplish this function. Since the bit synchronizers studied in this report operate in a digital fashion it appears that computer simulation of the bit synchronizer chosen will be required to determine overall performance and the approach of overall receiver simulation will be a fruitful one. Furthermore, affects due to multipath can be cranked into the model at a later time. Since this

effort may be costly it is important to decide whether other efforts to improve performance are not worthy of considering prior to modeling and simulating a system which will utlimately undergo change.

In developing sample data simulation techniques for the system it is recommended that the software be developed into three groups of subroutines. Group I subroutines would be those required to set up the simulation, Group II subroutines actually perform a function within the simulation and each subroutine will compute one value in its output waveform for each input sample point. Group III subroutines are those used by Group I.

The link may be represented by the following block diagram.

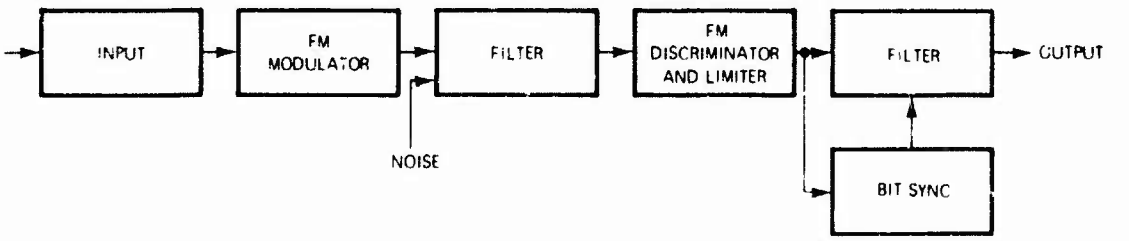

Figure VIII-13. RF Link.

The bilinear z transform can be used to develop sample data subroutines for making possible the realization of filters such as bandpass, lowpass symmetric and unsymmetric. The dependence of the sample data simulation on the RF carrier frequency can be eliminated by using analytic signal theory. This approach is important because the carrier frequency will be many times the highest baseband frequency resulting in a high sample rate and long computer run times if not eliminated.

REFERENCES

1. Guida, A. and Hecht, M., "Delay Modulation" Proc. IEEE, pp. 1314-1317, July 1969.

2. Lindsey, W. C., Synchronization Systems in Communication and Control , Prentice Hall, Inc., June 1972.

3. Lindsey, W. C., Simon, M. K., Telecommunication Systems Engineering, Prentice Hall, Englewood Cliffs, New Jersey, 1973.

4. Sage, A. P., McBride, A. L., "Optimum Estimation of Bit Synchronization," IEEE Transactions on Aerospace and Electronic Systems, Vol. AES-5, No. 3, pp. 525-536, May 1969.

5. Wintz, P. A., Luecke, E. J., "Performance of optimum and suboptimum synchronizers," IEEE Transactions of Communication Technology, Vol. COM-17, No. 3, pp. 380-389, June 1969.

6. Van Horn, J. H., "A theoretical synchronization system for use with noisy digital signals," IEEE Transactions on Communication Technology, Vol. COM-12, pp. 82-90, September 1964.

7. Wintz, P. A., Hancock, J. C., "An adaptive receiver approach to the time synchronization problem", IEEE Transactions on Communication Technology, Vol. COM-13, No. 1, pp. 90-96, March 1965.

8. Shaft, P., "Optimum design of the nonlinearity in signal tracking loops", Stanford Research Institute, Menlo Park, California, May 1968.

9. Stiffler, J. J., "On the selection of signals for phase-locked loops", IEEE Transactions on Communication Technology, Vol. COM-16, No. 2, pp. 239-244, April 1968.

10. Mengali, V., "A Self Bit Synchronizer Matched to the Signal Shape", IEEE Transactions on Aerospace and Electronic Systems, Vol. AES- No. 7, p. 686, July 1971.

11. Layland, J. W., "On optimal signals for phase-locked loops", IEEE Transactions on Communication Technology, Vol. COM-17, No. 5, pp. 526-531, October 1969.

12. Lindsey, W. C., and Tausworthe, R. C., "Digital Data-Transition Tracking Loops", Jet Propulsion Laboratory, Space Programs Summary 37-50, Vol. III, pp. 272-276, April 30, 1968.

13. Lindsey, W. C., and Anderson, T. O., "Digital Data-Transition Tracking Loops", paper presented at International Telemetry Conference, Oct. 8-10, 1968, Los Angeles, Calif.

14. Tausworthe, R. C., "Analysis and Design of the Symbol-Tracking Loop", Jet Propulsion Laboratory, Space Programs Summary 37-51, Vol. II, May 31, 1968.

15. Simon, M. K., "An Analysis of the Steady-State Phase Noise Performance of a Digital Data-Transition Tracking Loop", Jet Propulsion Laboratory Space Programs Summary, 37-55, Vol. III, pp. 54-62, February 28, 1969.

16. Simon, M. K., "Optimization of the Performance of a Digital Data Transition Tracking Loop", IEEE Transactions on Communication Technology, Vol. COM-18, no. 3, pp. 686-690, October 1970.

17. Layland, J. W., "Telemetry Bit Synchronization Loop", Jet Propulsion Laboratory Space Programs Summary 34-46, Vol. III, pp. 204-215.

18. Simon, M. K., "Nonlinear Analysis of an Absolute Value Type of Early-Late-Gate Bit Synchronizer", IEEE Transactions on Communication Technology, Vol. Com-18, no. 3, pp. 589-596, October 1970.

19. Rice, S. O., "Noise in FM Receivers," Proceedings, Symposium on Time Series Analysis, M Rosenblatt, Editor, New York, John Wiley and Sons, Inc., 1963.

20. Cohn, J., "A New Approach to the Analysis of FM Threshold Reception," Proceedings of the National Electronics Conference," pp. 221-236, 1956, Chicago, Ill.

21. Hill, E. R., "A Nonstatistical Treatment of FM Demodulator Noise," Naval Ordnance Laboratory Corona, NOLC Report 724, Sept. 15, 1967, Corona, Calif.

22. Schilling, D. L., Hoffman, E., Nelson, E. A., "Error Rates for Digital Signals Demodulated by an FM Discriminator," IEEE Trans. on Com. Tech, August, 1967.